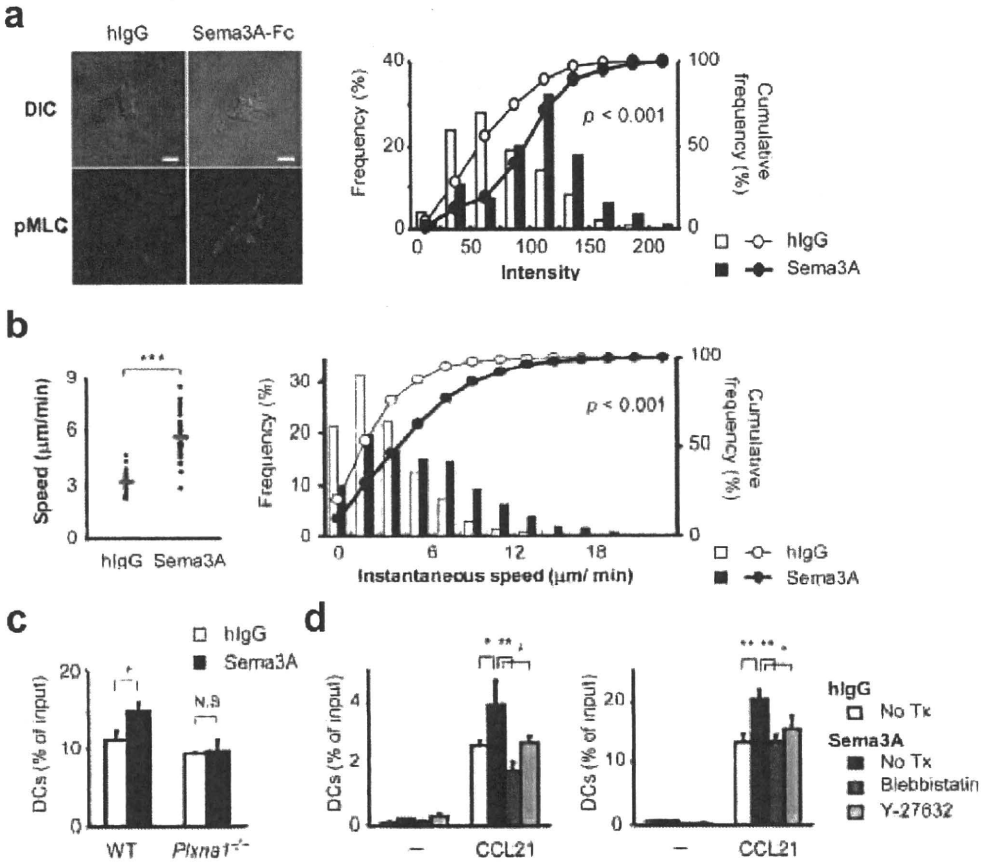

Figure 6. Sema3A induces phosphorylation of MLC and promotes actomyosin contraction

(**a**) Left: Confocal Z-stack imaging of DCs on fibronectin-coated coverslips treated with human IgG or Sema3A-Fc and stained with an anti-pMLC antibody plus an anti-rabbit-IgG-Cy3 (lower). Eight Z-stack images with an optical section separation (Z-interval) of 0.36 μm were were projected onto one single image. Scale bars, 10 μm (left). Right: Relative frequency distribution (bar chart) and cumulative frequency distribution (line chart) of the average intensities of dendrite regions in DCs that were stimulated with human IgG or Sema3A-Fc. $p<0.001$, by Mann-Whitney's *U* test. Data are representative of three independent experiments. (**b**) Mean velocities (left) and relative frequency distribution (bar chart) or cumulative frequency distribution (line chart) of the instantaneous speed (right) of a single DC in response to chemokines in the presence of human IgG or Sema3A-Fc in type I collagen matrices analyzed by time-lapse microscopy imaging and MetaMorph software. ***$p<0.001$, by Mann-Whitney's *U* test. Data are representative of three independent experiments. (**c**) Chemotaxis of wild-type or *Plxna1*$^{-/-}$ DCs in response to CCL21 in the presence of human IgG or Sema3A-Fc. DCs were added to the upper chambers of transwell assays with type I collagen. An overall difference between the groups was determined by one-way ANOVA. Post hoc multiple comparisons were made using Tukey's test. *$p<0.05$. (**d**) Chemotaxis of DCs treated with 50 μM blebbistatin or 30 μM Y-27632 for 30 min at 37°C and added to the upper chambers of transwells (pore size: 5 μm) layered with 3 mg/ml type I collagen (left) and a HMVEC-dLy monolayer (right) in response to CCL21 in the presence of human IgG or Sema3A-Fc in the upper chambers. An overall difference between the groups was determined by one-way ANOVA. Post hoc multiple comparisons were made using Tukey's test. *$p<0.05$, **$p<0.01$.

OPEN ACCESS Freely available online

PLoS one

Serum Anti-BPAG1 Auto-Antibody Is a Novel Marker for Human Melanoma

Takashi Shimbo[1], Atsushi Tanemura[2], Takehiko Yamazaki[1], Katsuto Tamai[1], Ichiro Katayama[2], Yasufumi Kaneda[1]*

1 Division of Gene Therapy Science, Osaka University Graduate School of Medicine, Osaka, Japan, 2 Department of Dermatology, Osaka University Graduate School of Medicine, Osaka, Japan

Abstract

Malignant melanoma is one of the most aggressive types of tumor. Because malignant melanoma is difficult to treat once it has metastasized, early detection and treatment are essential. The search for reliable biomarkers of early-stage melanoma, therefore, has received much attention. By using a novel method of screening tumor antigens and their auto-antibodies, we identified bullous pemphigoid antigen 1 (BPAG1) as a melanoma antigen recognized by its auto-antibody. BPAG1 is an auto-antigen in the skin disease bullous pemphigoid (BP) and anti-BPAG1 auto-antibodies are detectable in sera from BP patients and are used for BP diagnosis. However, BPAG1 has been viewed as predominantly a keratinocyte-associated protein and a relationship between BPAG1 expression and melanoma has not been previously reported. In the present study, we show that bpag1 is expressed in the mouse F10 melanoma cell line *in vitro* and F10 melanoma tumors *in vivo* and that BPAG1 is expressed in human melanoma cell lines (A375 and G361) and normal human melanocytes. Moreover, the levels of anti-BPAG1 auto-antibodies in the sera of melanoma patients were significantly higher than in the sera of healthy volunteers ($p<0.01$). Furthermore, anti-BPAG1 auto-antibodies were detected in melanoma patients at both early and advanced stages of disease. Here, we report anti-BPAG1 auto-antibodies as a promising marker for the diagnosis of melanoma, and we discuss the significance of the detection of such auto-antibodies in cancer biology and patients.

Citation: Shimbo T, Tanemura A, Yamazaki T, Tamai K, Katayama I, et al. (2010) Serum Anti-BPAG1 Auto-Antibody Is a Novel Marker for Human Melanoma. PLoS ONE 5(5): e10566. doi:10.1371/journal.pone.0010566

Editor: Vladimir Brusic, Dana-Farber Cancer Institute, United States of America

Received January 6, 2010; **Accepted** April 19, 2010; **Published** May 10, 2010

Funding: This work is supported by the Biomedical Cluster Kansai project, which is promoted by the Knowledge Cluster Initiative of the Ministry of Education, Culture, Sports, Science and Technology (http://www.mext.go.jp/). The funders had no role in study design, data collection and analysis, decision to publish, or preparation of the manuscript.

Competing Interests: The authors have declared that no competing interests exist.

* E-mail: kaneday@gts.med.osaka-u.ac.jp

Introduction

Melanoma is one of the most aggressive tumors due to its strong capacity to metastasize. In the United States, there were an estimated 62,480 new melanoma cases and 8,420 deaths caused by melanomas in 2008 [1]. Although the 5-year survival rate of patients with early stage localized melanoma is greater than 90%, survival rates drop to less than 20% once the melanoma has metastasized to distant sites [1]. In general, early diagnosis of cancers greatly improves the survival of patients. Therefore, great efforts have been made to screen tumor markers for early diagnosis. Several melanoma markers (e.g. gp100, MART-1 and tyrosinase) have been detected and proposed for immunotherapy approaches [2,3,4]. With regards to melanoma markers in serum, S100 protein, 5-S-cysteinyldopa and 6-hydroxy-5-methoxyindole-2-carboxylic acid can be useful although levels tend to be more up-regulated in advanced melanomas. As such, these particular markers are not suitable for the early detection of malignant melanoma [5]. Glypican-3 (GPC3), however, is overexpressed in melanoma and its serum concentration can serve as an early stage melanoma diagnostic marker [6,7]. Nevertheless, from a practical prospective, use of only one biomarker may lack sensitivity and specificity and diminish clinicopathologic value. The availability of multiple markers would make the diagnosis of melanoma more reliable, and thus there is a need to identify and assess additional melanoma markers.

In the present study, we developed a screening method to detect tumor markers recognized by auto-antibodies to these proteins in serum. Using this method, we found that bullous pemphigoid antigen 1 (BPAG1) was expressed in both melanoma cell lines and normal melanocytes. BPAG1 is a plakin family protein that anchors keratin filaments to hemidesmosomes [8]. Another protein BPAG2, a transmembranous collagen, is also expressed in the skin and is a component of hemidesmosomes [8]. Deletion of the *dst* gene, that encodes bpag1, disrupts hemidesmosomes structure, resulting in the failure of hemidesmosomes to associate with keratin filaments [9]. Both BPAG1 and BPAG2 can serve as auto-antigens in bullous pemphigoid (BP) [10,11,12]. Auto-antibodies to BPAG1 and BPAG2 maybe detected in the sera of BP patients, and assessment of antibody levels can be used for BP diagnosis and clinical management. While passive transfer experiments have shown that BPAG2 antibodies have pathogenic relevance to BP, the clinicopathological significance of BPAG1 antibodies, has not yet been fully elucidated [13]. It has been hypothesized that anti-BPAG1 auto-antibodies might interfere with hemidesmosome integrity, but this has not been proven [9].

Here, we show that the level of auto-antibodies against BPAG1 in the sera of melanoma patients, at both early and advanced

stages, was significantly higher than levels in the sera of healthy volunteers. These findings identify anti-BPAG1 auto-antibodies as a novel and promising tumor biomarker in the detection of melanoma.

Materials and Methods

Libraries, bacteria and helper phage

The human single-fold scFv libraries I + J (Tomlinson I + J), *E. coli* TG1 and HB2151, and KM13 helper phage were all kindly provided by the Medical Research Council (MRC). The scFv library was prepared as previously described [14]. The scFv library was cloned into the pIT2 expression vector, which contains a lac promoter and a pelB leader sequence upstream of the VH-$(G_4S)_3$-VL insert; the insert is followed by 6 ×His and myc tags, an amber stop codon and the gene encoding the pIII phage coat protein. Thus, in a suitable non-suppressor strain (HB2151), addition of isopropyl-thio-β-D-galactoside (IPTG) induces only scFv and not scFv–pIII fusion expression.

Mice

Female C57BL/6N mice (6 weeks old) were studied (Charles River Laboratories Japan, Inc., Japan) Animal experiments were performed in accordance with the guidelines of the Osaka University Graduate School of Medicine.

Cell lines and culture

Mouse melanoma cell line F10, mouse fibroblast cell line NIH-3T3, human melanoma cell lines A375, G361 and human epidermoid carcinoma A431 were obtained from the American Type Culture Collection (ATCC, USA). Normal human keratinocyte (NHK) cells and melanocyte (NHM) cells were obtained from Lonza (USA). F10, NIH-3T3, A375, G361 and A431 cells were maintained in Dulbecco's modified Eagle's medium (DMEM) (Nacalai Tesque Inc., Japan). DMEM was supplemented with 10% fetal bovine serum (FBS) (Biowest, France), 100 units/ml penicillin and 0.1 mg/ml streptomycin (penicillin-streptomycin mixed solution) (Nacalai). NHK and NHM cells were maintained in keratinocyte growth medium (KGM) (Lonza) and melanocyte growth medium (MGM-4) (Lonza), respectively.

Preparation of tumor lysates and the isolation of sera from tumor-bearing mice

F10 cells (5×10^6) were intradermally injected into the backs of C57BL/6N mice. After 4 weeks, tumors were excised, and protein was extracted using T-PER Tissue Protein Extraction Reagent (Pierce, USA), according to the manufacturer's instructions. At the same time as the tumor excision, whole blood was collected, and the sera were isolated using Capiject Capillary Blood Collection Tubes (Terumo Corp., Japan).

In vivo screening of tumor-homing phages and isolation of the tumor-binding scFv

F10 cells (5×10^6) were intradermally injected into the backs of C57BL/6N mice. After tumors reached 7 to 8 mm in diameter, we injected the phage library (1×10^{13} CFU) dissolved in 100 µl saline into the tail veins of tumor-bearing mice. After 15 min, the animals were sacrificed by an overdose of anesthetic and perfused via the heart with 100 ml of PBS [15]. Next, the tumor tissue was snap-frozen in liquid nitrogen and homogenized in a mortar. Tumor-homing phages were eluted by using 500 µl of 0.1 M glycine (pH 2.2) for 15 min, and then the solution was neutralized with 50 µl of 2 M Tris-HCl (pH 8). Next, 50 µL of Protein A (GE Healthcare, USA) was added to the neutralized phage solution, and the mixture was rotated for 1.5 h at 4°C. After washing with PBS to remove unbound phages, phages bound to protein A were used to infect log-phase HB2151 for 1 h at 37°C; then, the cells were plated on 2×YT agar plates containing 100 µg/ml carbenicillin. After 16 h of incubation at 37°C, a nitrocellulose membrane soaked in 100 mM IPTG (Takara Bio Inc., Japan) for 10 min was placed on the 2×YT plate for 4 h at 37°C. The plate was stored at 4°C as a master plate for *E.coli* recovery. The membrane was washed 3 times with PBS containing 0.1% tween 20 and blocked 30 min with PBS containing 5% skim milk (Nacalai). Then, the membrane was incubated with tumor lysate followed by tumor-bearing mouse serum. The complexes of auto-antibodies bound to tumor proteins were detected with the anti-mouse IgG horseradish peroxidase-conjugated antibody (GE Healthcare) followed by ECL Western Blotting Kit (GE Healthcare).

Identification of tumor antigen with MALDI-TOF mass spectrometry

Positive clones that were recovered from the stored 2×YT agar plate were re-plated onto a fresh 2×YT agar plate and incubated for 16 h at 37°C. Next, a nitrocellulose membrane soaked with 100 mM IPTG was placed onto the 2×YT agar plate for 4 h at 37°C. After washing with PBS containing 0.1% tween 20, the membrane was blocked 30 min with 0.5% polyvinylpyrrolidone K30 (Nacalai), and then the membrane was incubated with tumor lysate. The scFv-tumor protein complexes were stained with 0.5% ponceau (Wako Pure Chemical Industries, Ltd., Japan)/5% acetic acid in distilled water, and the membrane around the area was excised. The protein on the excised membrane was digested with 100 ng/ml trypsin (Sigma-Aldrich, USA)/40 mM ammonium bicarbonate (Nacalai) for 6 h at 37°C. Then, the solution was dried up, and saturated α-cyano-4-hydroxy cinnamic acid (Wako), 1% trifluoroacetic acid, and 50% acetonitrile was added. After desalting with a ZipTip C18, the solution was analyzed using an Ultraflex MALDI-TOF/TOF instrument (Bruker Daltonik, Germany). The mass spectrometry data were analyzed with the Mascot search engine (http://www.matrixscience.com).

RT-PCR and real-time PCR

RNA was extracted using Isogen (Nippon Gene, Japan), and 1 µg of total RNA was converted to cDNA with SuperScript III (Invitrogen, USA), according to the manufacturer's instructions. Mouse bullous pemphigoid antigen 1 (bpag1), TBC1 domain family member 13 (tbc1d13), uncharacterized protein C7orf30 homolog (c7orf30), and β-actin were amplified using SYBR Premix Ex Taq (Takara Bio) and an ABI Prism 7900 sequence detector (Applied Biosystems, USA). Human BPAG1, BPAG2, and β-actin were amplified with TaKaRa Ex Taq Hot Start Version, and PCR products were analyzed by electrophoresis on 1% agarose gels. All procedures were performed according to the manufacturer's instructions.

The primers were as follows:

Mouse bpag1-f:5′- TTGGAACAGACCTGGAGACC-3′
Mouse bpag1-r:5′- GTTCAGCCTTTCCATTTCCA-3′
Mouse tbc1d13-f:5′- AGGCCAACATGGGTGTATTC -3′
Mouse tbc1d13-r:5′- AGGGTTTGGGTTCAGAGGAT-3′
Mouse c7orf30-f:5′- GAGGGGAAGGACGCTGAC -3′
Mouse c7orf30-r:5′- TGGAAGCATCAAATGGATCA-3′
Mouse β-actin-f:5′- CCACTGCCGCATCCTCTTCC-3′
Mouse β-actin-r:5′- CTCGTTGCCAATAGTGATGACCTG -3′
Human BPAG1-f:5′- CCAGCCCGGTTAACTATTGA -3′

Human BPAG1-r:5′- TGGCAGAGCTGTAAGATCCA-3′
Human BPAG2-f:5′- GCTGGAGATCTGGATTACAATGA-3′
Human BPAG2-r:5′- CCTTGCAGTAGGCCCTGA-3′
Human β-actin -f:5′- GAGCTACGAGCTGCCTGACG-3′
Human β-actin -r:5′- GTAGTTTCGTGGATGCCACAG-3′

Detection of BPAG1 by Immunoprecipitation (IP) and Western blotting

Cells (1×10^7) were trypsinized, washed in cold PBS and resuspended in 500 µl RIPA buffer. IP of total cell lysates were incubated with anti-BPAG1 antibody (sc-13776) (Santa Cruz Biotechnology Inc., USA) or normal goat IgG (Santa Cruz) for 1 h followed by protein G agarose (GE Healthcare) overnight. SDS-PAGE and Western blotting were performed, as previously described [16] with anti-BPAG1 antibody. After incubation with HRP conjugated anti-goat IgG (R&D systems, USA), signals were detected with ECL Western Blotting Detection Regents (GE Healthcare) according to the manufacturer's instructions.

Quantification of BPAG1 auto-antibodies in sera

Approval for this study was obtained from the Institutional Review Board of the Osaka University Hospital (#08312). Written informed consent was obtained from all participants before the study. We collected sera from 55 melanoma patients and 27 healthy volunteers. The malignant melanoma patients studied here consisted of 24 men and 31 women with an average age of 62.6 years (range, 22 to 86 years); 13 had stage 0 (*in situ*) or stage I; 5 had stage II; 11 had stage III; 26 had stage IV. The healthy volunteers consisted of 15 men and 12 women with an average age of 31.6 years (range, 24 to 49years). The sera samples were stored at −30°C prior to use and the serum levels of anti-BPAG1 auto-antibodies were determined using a BP230 ELISA kit (MBL, Japan) according to the manufacturer's instructions. The INDEX was calculated as follows; INDEX = (sample absorbance − negative control absorbance [INDEX = 0])/(positive control absorbance [INDEX = 100] - negative control absorbance) ×100 [17]. The Mann-Whitney U test was used to determine statistical significance, and $p<0.05$ was considered statistically significant.

Results

Identification of bpag1 as a tumor antigen recognized by auto-antibodies

An overview of the screening procedure is shown in Figure 1. We performed the screening on mouse F10 melanoma cell lines. The tumor-homing phages were collected by *in vivo* biopanning in tumor-bearing mice. The phages were used to infect HB2151 for scFv expression and plated on a 2×YT agar plate. After 16 h, scFv expression was induced with IPTG, and the resulting scFvs were transferred onto a nitrocellulose membrane. The membrane was incubated with F10 melanoma tumor lysate followed by F10 tumor-bearing mouse serum. The scFv-tumor protein complexes on the nitrocellulose membrane were detected with the auto-antibodies in the serum collected from the tumor-bearing mice (Figure 2A). We performed the screening procedure several times and selected high-signal clones, distinct from background signals, for further experiments. Next, we analyzed the proteins that were detected with auto-antibodies by performing MALDI-TOF mass spectrometry, and we identified 8 potential melanoma marker candidates with statistical significance ($p<0.05$) (Figure 2B). The candidates were ordered according to the expectation value, which is the expected frequency of the matches to be obtained from mass spectrometry merely by chance. We compared the expression of the 8 candidates among NIH-3T3 cells, F10 melanoma cells and F10 melanoma tumors by real-time PCR. Bpag1, tbc1d13 and c7orf30 were expressed at much higher levels in F10 melanoma cells (7.0-, 3.1- and 1.9-fold, respectively) and F10 melanoma tumors (10.9-, 4.2- and 6.3-fold, respectively) as compared to NIH-3T3 cells (Figure 2C); the expression levels of the remaining 5 candidates in melanoma cells and tumors were less than the expression level in NIH-3T3 cells (data not shown). Among the three candidates, we selected bpag1 for further investigation because bpag1 was expressed most abundantly in F10 melanoma cells and tumors, and is known to have a restricted tissue expression pattern, including skin, brain and muscle [18].

Differential expression of BPAG1 and BPAG2 in normal human melanocytes and human melanoma cell lines

We used RT-PCR to confirm the expression of BPAG1 in human melanomas. BPAG1 is expressed in normal human keratinocytes and is a component of hemidesmosomes along with BPAG2. Thus, we used normal human keratinocytes as a positive control for both these proteins. We identified BPAG1 expression in human melanoma cell lines (A375 and G361) and normal human melanocytes (Figure 3A). However, we did not detect BPAG2 expression in the human melanoma cell lines or normal human melanocytes (Figure 3A). We also detected BPAG1 protein in A375 and G361 by IP-western blotting (Figure 3B).

Quantification of anti-BPAG1 auto-antibodies in sera

Auto-antibodies against BPAG1 are found in sera from BP and therefore BPAG1 maybe a highly immunogenic protein. We hypothesized that the human immune system might generate auto-antibodies against BPAG1 expressed in human melanomas. To assess this possibility, we collected sera from 55 melanoma patients and 27 healthy volunteers and quantified the serum levels of anti-BPAG1 auto-antibodies by ELISA (Figure 4A). The average (±S.E.M.) INDEX value of the control group and the melanoma group was 1.64 (±0.27) and 3.47 (±0.40), respectively. We classified melanoma patients as follows: *in situ*, stage I or stage II patients were "early" (n = 18), and stage III or stage IV patients were "advanced" (n = 37). The levels of anti-BPAG1 auto-antibodies were much higher in both early and advanced stage melanoma patients ($p<0.01$) as compared to the healthy volunteers (Figure 4B). The average INDEX value (±S.E.M.) for the early and advanced melanoma patients was 4.14 (±0.83) and 3.15 (±0.43), respectively. Next, we evaluated the possibility of using anti-BPAG1 auto-antibodies as a melanoma detection marker. The maximum INDEX value in healthy volunteers (4.64) was defined as the cut off level. Applying these criteria, the positive rates of serum anti-BPAG1 auto-antibodies were 23.6% in total melanoma patients (13/55), 33.3% in early stage melanoma patients (6/18), and 18.9% in advanced stage melanoma patients (7/37) (Table 1). We also conducted indirect immunofluorescence studies using 4 melanoma patients' sera and demonstrated that IgG antibodies produced in patients reacted with skin basement membrane zone with variability in staining intensive (down to a dilution of 1:160).

Discussion

In the present study, we developed a novel screening method for detecting tumor biomarkers. Our method is similar to SEREX in that we use serum containing anti-tumor auto-antibodies, but unlike SEREX, however, our method does not require a cDNA library from tumor tissue [19,20,21]. We anticipate that our method has clinical applicability, because it can be applied to human patients by modifying the method to select tumor-homing

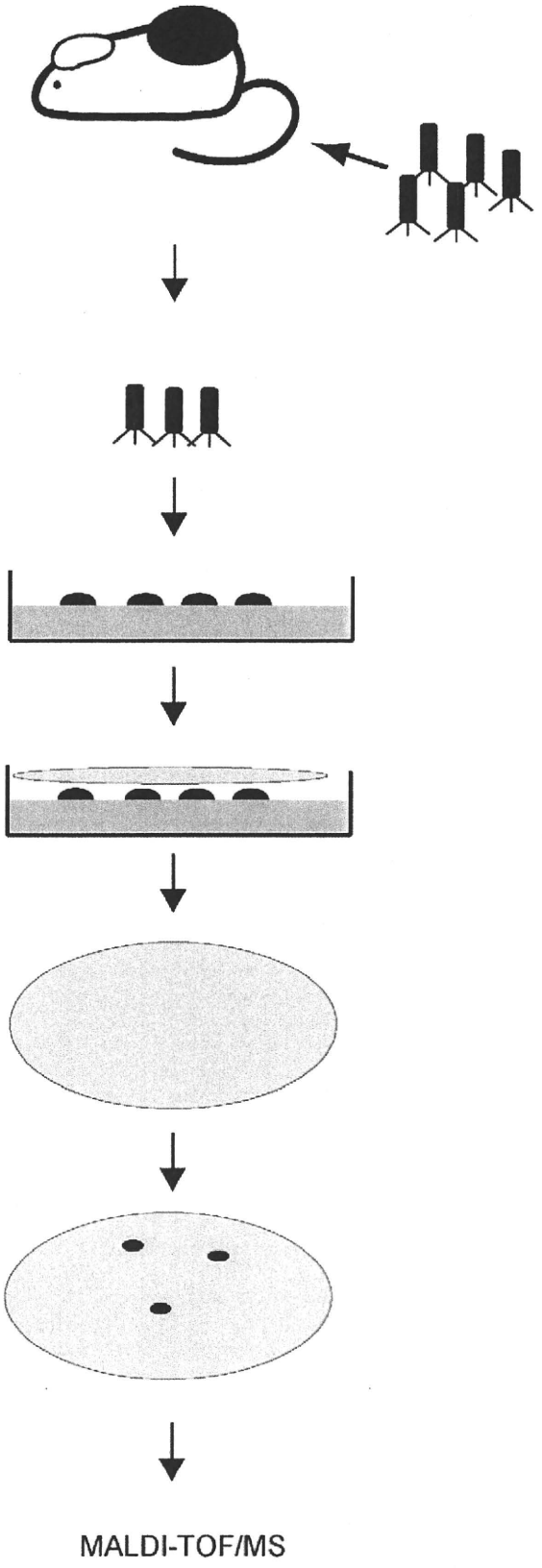

Figure 1. Overview of the rapid method for isolating auto-antibody against tumor-associated antigen (TAA) using a scFv library. The tumor-homing scFv-presenting phages were collected from tumors that were injected with a scFv library. The collected phages were infected to

HB2151 for scFv secretion. The secreted scFvs from HB2151 were transferred to nitrocellulose membranes by colony lift. The membranes were incubated with tumor lysate followed by serum from a tumor-bearing mouse. The scFv-tumor protein complex was detected by auto-antibodies. The complex was digested into peptide by trypsin and analyzed using MALDI-TOF mass spectrometry for identification.
doi:10.1371/journal.pone.0010566.g001

phage. In this report, we selected tumor-homing phage using tumor-bearing mice, but it is also possible to use tumor specimens [22]. Moreover, the phage screening could be conducted in human cancer patients without any detectable toxicity [23]. This method therefore has the potential to identify the most suitable tumor antigens for diagnosis or vaccination.

Nevertheless, our method did not detect previously identified melanoma antigens, such as gp100, tyrosinase, TRP-1 and TRP-2; instead, it detected completely different proteins. Gp100, tyrosinase, and TRP-2 were identified previously as melanoma antigens recognized by cytotoxic T cells from cancer patients, and TRP-1 was identified as a melanoma antigen recognized by IgG antibodies in the serum of a melanoma patient [24]. The epitopes of these antigens can efficiently activate tumor immunity, and they have been developed for cancer immunotherapy trials [25]. Although auto-antibodies to these melanoma antigens were detected in the sera of melanoma patients, the antigens were not frequently identified in sera from melanoma patients [26,27,28]. A possible explanation might be that auto-antibodies to such melanoma antigens exist in the sera of melanoma patients, but lack sensitivity or are present at low titers. Proteins identified by our screening method, however, have the potential to elicit the production of auto-antibodies in tumor-bearing individuals. In other words, our screening method may detect highly immunogenic proteins. Thus, it can be an effective tool for identifying detection markers in serum.

Given the differences in immune systems between mice and human, it is possible that the positive results screened in mice might

A

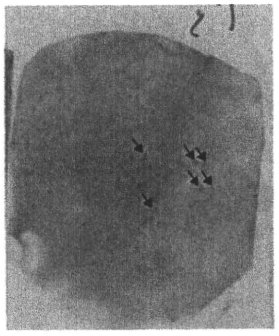

B

protein	expect
Diamine acetyltransferase 2 (sat2)	0.0021
Bullous pemphigoid antigen 1, isoforms1/2/3/4 (bpag1)	0.0036
voltage-dependent calcium channel subunit alpha2/delta3 (cacna2d3)	0.028
LRR and PYD domains-containing protein F4 (nal4f)	0.038
TBC1 domain family member 13 (tbc1d13)	0.04
nibrin	0.04
Uncharacterized protein C7orf30 homolog (c7orf30)	0.045
serine/threonine-protein kinase (plk2)	0.047

C

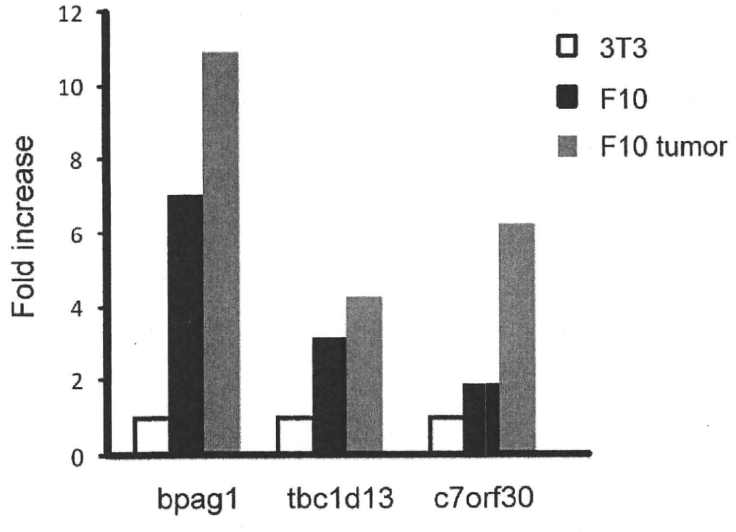

Figure 2. Identification of bpag1 as a tumor antigen recognized by auto-antibodies. (A) An example of the screening output. ScFv-tumor antigen complex was detected with auto-antibodies in tumor-bearing mouse serum. (B) Eight candidates were identified by MALDI-TOF mass spectrometry with statistical significance ($p<0.05$); expect = expectation value. (C) Comparison of bpag1, tbc1d13 and c7orf30 expression in NIH-3T3 cells (white bar), F10 melanoma cells (black bar) and F10 melanoma tumors (grey bar) by SYBR Green real-time PCR.
doi:10.1371/journal.pone.0010566.g002

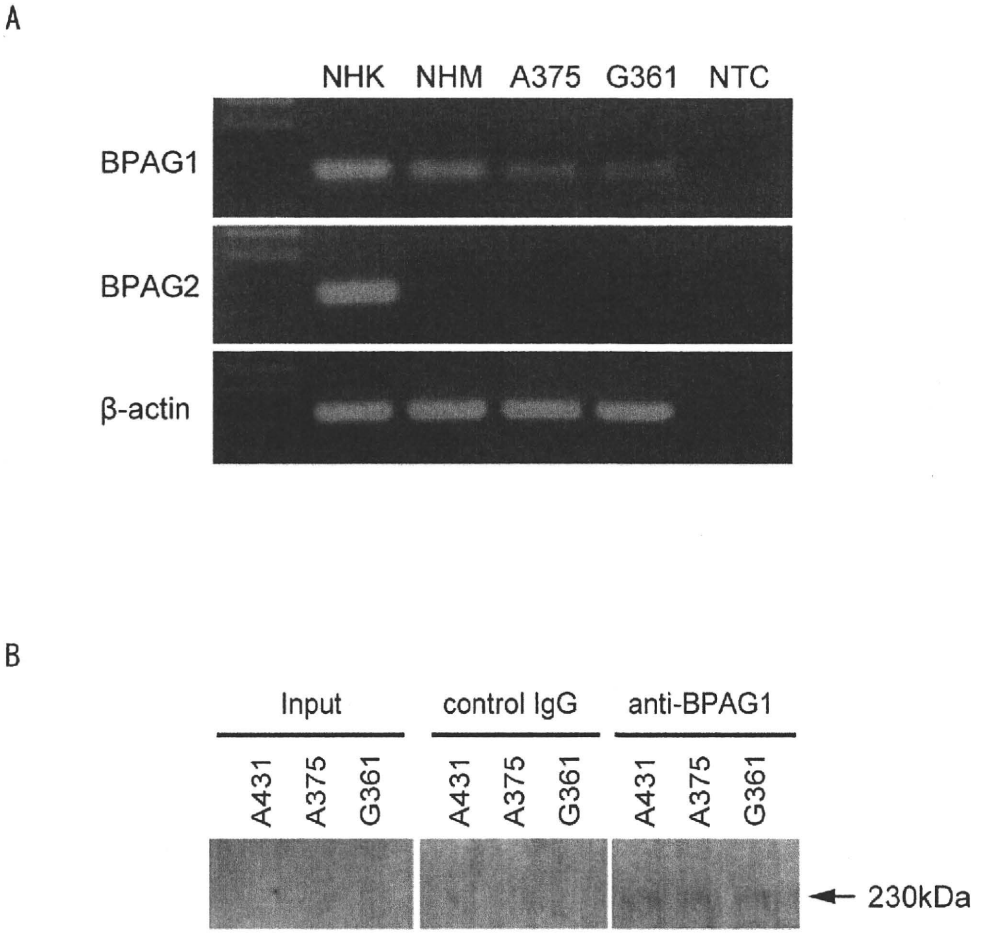

Figure 3. Expression of BPAG1 in normal human melanocytes and human melanoma cell lines. (A) The expression of BPAG1 and BPAG2 mRNA was quantified by RT-PCR in normal human melanocytes (NHM) and human melanoma cell lines A375 and G361. Normal human keratinocyte (NHK) mRNA was used as a positive control. β-actin was amplified as a loading control for cDNA. NTC; no template control. (B) The expression of BPAG1 protein was detected by IP-western blotting in human melanoma cell lines A375 and G361. A431 was used as positive control for BPAG1. The arrow indicates BPAG1.
doi:10.1371/journal.pone.0010566.g003

be negative in humans. Ideally, screening procedures for auto-antibodies need to be performed in human melanoma patients. However, although the phage screening has been conducted in human cancer patients without any detectable toxicity, the method is still at a clinical trial stage [23]. It is therefore not yet straightforward or practicable to conduct phage screening in humans. With regards to our studies, screening mice also has the advantages of repeatability and uniformity of samples. On the other hand, it is difficult to conduct repeated screening in human cancer patients. Moreover, since the background of all the murine samples is uniform in our screening, any consistently positive result from repeated screenings will be highly reliable as tumor markers. In contrast, since the tumor stages and immunological states of patients are diverse, the results of screening using human patient sera would need extensive re-validation work.

We also showed that BPAG1 is expressed in human melanoma cell lines and that auto-antibodies against BPAG1 can be a potent melanoma marker. BPAG1 is expressed in normal keratinocytes within hemidesmosomes in association with BPAG2 and other proteins [8]. We did not detect any BPAG2 expression in human melanoma cell lines and melanocytes, and thus BPAG1 may have distinct functions in melanomas and melanocytes. BPAG1 is also expressed in some neurons and is involved in axonal neurofilament aggregation and axonal microtubule disorganization [29,30]. The expression of BPAG1 in a human epidermoid carcinoma cell line (A431) and mammary ductal carcinoma *in situ* has also been confirmed [31,32]. Thus BPAG1 may have an as yet undefined role related to tumorigenesis or tumor progression; overexpression and suppression of BPAG1 in melanocytes and melanomas will be necessary to determine this in more detail.

Some patients with melanoma develop vitiligo-like white patches, known as melanoma-associated hypopigmentation (MAH), on their skin [33]. Interestingly, the presence of vitiligo in melanoma patients may correlate with improved prognosis [34,35]. Such patients with vitiligo could have more effective immunity against melanoma than patients without vitiligo. In general, the appearance of autoimmune phenomena improves the outcome of cancer patients [36]. However, such autoimmune phenomena are suppressed in most cancer patients by regulatory T (Treg) cells [37]. Treg cells inhibit $CD8^+$ and $CD4^+$ T cells, which are major components of cancer immunosuppression [38,39]. The depletion of Treg cells from tumor-bearing mice promotes tumor regression [38,39]. Interestingly, auto-antibodies

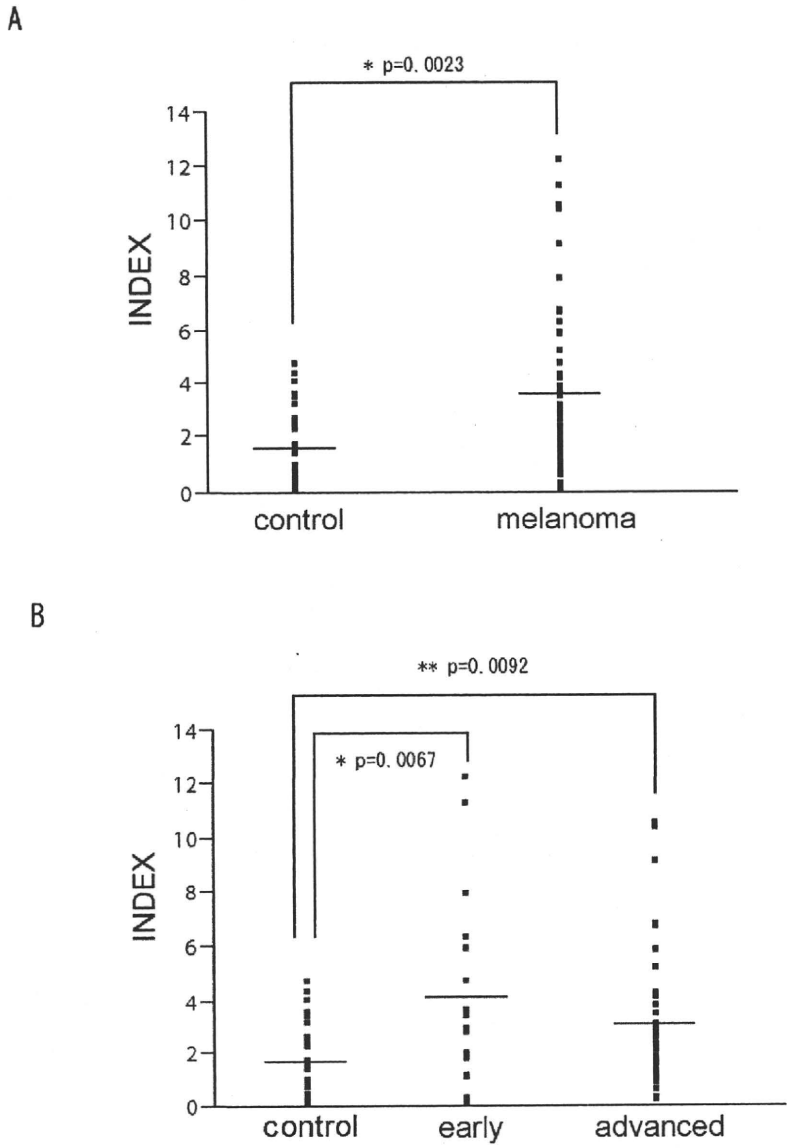

Figure 4. Quantification of anti-BPAG1 auto-antibodies in melanoma patients. (A) The levels of anti-BPAG1 auto-antibodies in sera collected from healthy volunteers and melanoma patients were quantified using a MESACUP BP230 ELISA Kit. The INDEX values were plotted and the average INDEX values as shown (±S.E.M.) for control subjects (1.64±0.27) and melanoma patients (3.47±0.40). (B) The melanoma patients were classified using the American Joint Committee on Cancer (AJCC) 2002 staging criteria. *In situ*, stage I or stage II patients were categorized as "early", while stage III or stage IV patients were categorized as "advanced". The average INDEX values (±S.E.M.) of early and advanced melanoma patients were 4.14±0.83 and 3.15±0.43, respectively; the bars indicate the average INDEX value.
doi:10.1371/journal.pone.0010566.g004

were detected in mice showing tumor regression [38]. The efficiency of Treg-cell depletion may correlate with the emergence of auto-antibodies. Thus, the presence of anti-BPAG1 auto-antibodies may correlate with the occurrence of autoimmune responses in melanoma patients. By quantification of anti-BPAG1 auto-antibodies, it maybe possible to predict the immune status of cancer patients. In theory, immunotherapy against melanoma, therefore, might be more effective for patients with anti-BPAG1 auto-antibodies than those without antibodies.

We showed that BPAG1 is expressed both in melanocytes and melanomas. Since BPAG1 expression is maintained throughout the stages of melanoma tumorigenesis, BPAG1 auto-antibodies can be created even in the early stage of melanoma. We showed that the levels of anti-BPAG1 auto-antibodies are higher in melanoma patients at both early and advanced stages than in healthy volunteers (Figure 4 and Table 1). This result suggests that anti-BPAG1 auto-antibodies can be present in early stage melanoma, i.e. before it metastasizes. Thus, anti-BPAG1 auto-antibodies have the potential to be a promising melanoma biomarker. To test this hypothesis, we are planning to conduct a larger clinical study.

To the best of our knowledge, this report is the first to show BPAG1 expression in human melanomas and melanocytes and to highlight the potential of anti-BPAG1 auto-antibodies in the serum

Table 1. Positive rates of serum anti-BPAG1 auto-antibody in stage-classified melanoma patients.

stage	total sample number	BPAG1 auto-antibody positive	%
early	18	6	33.3
advanced	37	7	18.9
total	55	13	23.6

The maximum INDEX value in healthy volunteers (4.64) was defined as the cut off level. The patients were classified by using the American Joint Committee on Cancer (AJCC) 2002 staging criteria. *In situ*, stage I or stage II patients were classified as "early", while stage III or stage IV patients were classified as "advanced".
doi:10.1371/journal.pone.0010566.t001

.as a marker of melanoma. We also demonstrated the effectiveness of our screening method. We will continue to develop this method into a more sophisticated method that can be used clinically. To validate the use of anti-BPAG1 auto-antibodies for melanoma diagnosis, we need to clarify the function of BPAG1 in melanoma and the mechanism of auto-antibody creation. These studies will be fundamental in assessing whether BPAG1 auto-antibodies can have an impact on improving the prognosis of melanomas.

Author Contributions

Conceived and designed the experiments: TS YK. Performed the experiments: TS. Analyzed the data: TS AT KT. Contributed reagents/materials/analysis tools: AT TY IK. Wrote the paper: TS YK.

References

1. Jemal A, Siegel R, Ward E, Hao Y, Xu J, et al. (2008) Cancer statistics, 2008. CA Cancer J Clin 58: 71–96.
2. Bosserhoff AK (2006) Novel biomarkers in malignant melanoma. Clin Chim Acta 367: 28–35.
3. Gould Rothberg BE, Bracken MB, Rimm DL (2009) Tissue biomarkers for prognosis in cutaneous melanoma: a systematic review and meta-analysis. J Natl Cancer Inst 101: 452–474.
4. Ohsie SJ, Sarantopoulos GP, Cochran AJ, Binder SW (2008) Immunohistochemical characteristics of melanoma. J Cutan Pathol 35: 433–444.
5. Brochez L, Naeyaert JM (2000) Serological markers for melanoma. Br J Dermatol 143: 256–268.
6. Ikuta Y, Nakatsura T, Kageshita T, Fukushima S, Ito S, et al. (2005) Highly sensitive detection of melanoma at an early stage based on the increased serum secreted protein acidic and rich in cysteine and glypican-3 levels. Clin Cancer Res 11: 8079–8088.
7. Nakatsura T, Kageshita T, Ito S, Wakamatsu K, Monji M, et al. (2004) Identification of glypican-3 as a novel tumor marker for melanoma. Clin Cancer Res 10: 6612–6621.
8. Kasperkiewicz M, Zillikens D (2007) The pathophysiology of bullous pemphigoid. Clin Rev Allergy Immunol 33: 67–77.
9. Guo L, Degenstein L, Dowling J, Yu QC, Wollmann R, et al. (1995) Gene targeting of BPAG1: abnormalities in mechanical strength and cell migration in stratified epithelia and neurologic degeneration. Cell 81: 233–244.
10. Labib RS, Anhalt GJ, Patel HP, Mutasim DF, Diaz LA (1986) Molecular heterogeneity of the bullous pemphigoid antigens as detected by immunoblotting. J Immunol 136: 1231–1235.
11. Mutasim DF, Takahashi Y, Labib RS, Anhalt GJ, Patel HP, et al. (1985) A pool of bullous pemphigoid antigen (s) is intracellular and associated with the basal cell cytoskeleton-hemidesmosome complex. J Invest Dermatol 84: 47–53.
12. Stanley JR, Hawley-Nelson P, Yuspa SH, Shevach EM, Katz SI (1981) Characterization of bullous pemphigoid antigen: a unique basement membrane protein of stratified squamous epithelia. Cell 24: 897–903.
13. Liu Z, Diaz LA, Troy JL, Taylor AF, Emery DJ, et al. (1993) A passive transfer model of the organ-specific autoimmune disease, bullous pemphigoid, using antibodies generated against the hemidesmosomal antigen, BP180. J Clin Invest 92: 2480–2488.
14. de Wildt RMT, Mundy CR, Gorick BD, Tomlinson IM (2000) Antibody arrays for high-throughput screening of antibody-antigen interactions. Nat Biotechnol 18: 989–994.
15. Lee L, Garrood T, Pitzalis C (2007) In vivo phage display selection in the human/SCID mouse chimera model for defining synovial specific determinants. Methods Mol Med 136: 369–394.
16. Tanaka M, Shimbo T, Kikuchi Y, Matsuda M, Kaneda Y (2010) Sterile alpha motif containing domain 9 is involved in death signaling of malignant glioma treated with inactivated Sendai virus particle (HVJ-E) or type I interferon. Int J Cancer 126: 1982–1991.
17. Nishie W, Sawamura D, Goto M, Ito K, Shibaki A, et al. (2007) Humanization of autoantigen. Nat Med 13: 378–383.
18. Okumura M, Yamakawa H, Ohara O, Owaribe K (2002) Novel alternative splicings of BPAG1 (bullous pemphigoid antigen 1) including the domain structure closely related to MACF (microtubule actin cross-linking factor). J Biol Chem 277: 6682–6687.
19. Sahin U, Tureci O, Schmitt H, Cochlovius B, Johannes T, et al. (1995) Human neoplasms elicit multiple specific immune responses in the autologous host. Proc Natl Acad Sci U S A 92: 11810–11813.
20. Li G, Miles A, Line A, Rees RC (2004) Identification of tumour antigens by serological analysis of cDNA expression cloning. Cancer Immunol Immunother 53: 139–143.
21. Gunawardana CG, Diamandis EP (2007) High throughput proteomic strategies for identifying tumour-associated antigens. Cancer Lett 249: 110–119.
22. Sun Y, Shukla GS, Weaver D, Pero SC, Krag DN (2009) Phage-display selection on tumor histological specimens with laser capture microdissection. J Immunol Methods 347: 46–53.
23. Krag DN, Shukla GS, Shen GP, Pero S, Ashikaga T, et al. (2006) Selection of tumor-binding ligands in cancer patients with phage display libraries. Cancer Res 66: 7724–7733.
24. Kawakami Y, Rosenberg SA (1997) Human tumor antigens recognized by T-cells. Immunol Res 16: 313–339.
25. Rosenberg SA, Yang JC, Restifo NP (2004) Cancer immunotherapy: moving beyond current vaccines. Nat Med 10: 909–915.
26. Huang SK, Okamoto T, Morton DL, Hoon DS (1998) Antibody responses to melanoma/melanocyte autoantigens in melanoma patients. J Invest Dermatol 111: 662–667.
27. Forgber M, Trefzer U, Sterry W, Walden P (2009) Proteome serological determination of tumor-associated antigens in melanoma. PLoS One 4: e5199.
28. Ehlken H, Schadendorf D, Eichmuller S (2004) Humoral immune response against melanoma antigens induced by vaccination with cytokine gene-modified autologous tumor cells. Int J Cancer 108: 307–313.
29. Brown A, Bernier G, Mathieu M, Rossant J, Kothary R (1995) The mouse dystonia musculorum gene is a neural isoform of bullous pemphigoid antigen 1. Nat Genet 10: 301–306.
30. Young KG, Kothary R (2007) Dystonin/Bpag1-A link to what? Cell Motil Cytoskeleton 64: 897–905.
31. Lee CW (2000) An extract of cultured A431 cells contains major tissue antigens of autoimmune bullous diseases. Br J Dermatol 143: 821–823.
32. Schuetz CS, Bonin M, Clare SE, Nieselt K, Sotlar K, et al. (2006) Progression-specific genes identified by expression profiling of matched ductal carcinomas in situ and invasive breast tumors, combining laser capture microdissection and oligonucleotide microarray analysis. Cancer Res 66: 5278–5286.
33. Ram M, Shoenfeld Y (2007) Harnessing Autoimmunity (Vitiligo) to Treat Melanoma: A Myth or Reality? Ann N Y Acad Sci 1110: 410–425.
34. Bystryn JC (1989) Serum antibodies in vitiligo patients. Clin Dermatol 7: 136–145.
35. Oyarbide-Valencia K, van den Boorn JG, Denman CJ, Li M, Carlson JM, et al. (2006) Therapeutic implications of autoimmune vitiligo T cells. Autoimmun Rev 5: 486–492.
36. Gogas H, Ioannovich J, Dafni U, Stavropoulou-Giokas C, Frangia K, et al. (2006) Prognostic significance of autoimmunity during treatment of melanoma with interferon. N Engl J Med 354: 709–718.
37. Kim R, Emi M, Tanabe K (2006) Cancer immunosuppression and autoimmune disease: beyond immunosuppressive networks for tumour immunity. Immunology 119: 254–264.
38. Ko K, Yamazaki S, Nakamura K, Nishioka T, Hirota K, et al. (2005) Treatment of advanced tumors with agonistic anti-GITR mAb and its effects on tumor-infiltrating Foxp3+CD25+CD4+ regulatory T cells. J Exp Med 202: 885–891.
39. Wei WZ, Jacob JB, Zielinski JF, Flynn JC, Shim KD, et al. (2005) Concurrent induction of antitumor immunity and autoimmune thyroiditis in CD4+ CD25+ regulatory T cell-depleted mice. Cancer Res 65: 8471–8478.

tions, no perforation was documented and no foreign material was identified.

The diagnosis of granuloma annulare was therefore made. Follow-up after six months revealed a very good cosmetic result and no recurrence was observed. Lesions of the right ear were excised and histological examination confirmed the same diagnosis.

Lesions of granuloma annulare localized to the external ear are very rare. To our knowledge, this is the sixth case reported. While most cases of granuloma annulare occur in females, the five reports of granuloma annulare in the external ear were in men [1, 4-6]. Although the exact reason why these lesions appear localized to the external ear is unknown, there seems to be some relation with trauma [4]. Differential diagnosis must include, in addition to epidermal cysts, sarcoidosis, chondrodermatitis nodularis helicis, intracartilagenous pseudocyst of the auricle, "cauliflower ears" from recurrent hematomas and rheumatoid nodules. Some of these diseases are associated with trauma, which was not present in our clinical report. The final diagnosis was established by the histological examination. This case illustrates that a careful clinical assessment and appropriate biopsy must be performed when diagnosing lesions of the outer ear. Granuloma annulare should be considered in the differential diagnosis of nodular lesions at this site. ■

Acknowledgements. *Conflict of interest: none. Funding sources: none.*

[1]Department of Dermatology,
Centro Hospitalar de Lisboa Central,
Alameda Santo António
dos Capuchos,
1169-050 Lisboa, Portugal
[2]Centro de Dermatologia
Médico-Cirúrgica de Lisboa,
Lisbon, Portugal
<joanadiascoelho@hotmail.com>

Joana DIAS COELHO[1]
Isabel VIANA[2]
Susete CORREIA[2]

1. Raghava N, Mitchard JR, Youngs RP. Granuloma annulare presenting as multiple nodules on the pinna. *J Laryngol Otol* 2004; 118: 640-2.
2. Marcus DV, Mahmoud BH, Hamzavi IH. Granuloma annulare treated with rifampin, ofloxacin, and minocycline combination therapy. *Arch Dermatol* 2009; 145: 787-9.
3. Farrar CW, Bell HK, Dobson CM, Sharpe GR. Perforating granuloma annulare presenting on the ears. *Br J Dermatol* 2002; 147: 1026-8.
4. Dompmartin A. Nodules of the external ear. *Ann Dermatol Venereol* 1999; 126: 261-6.
5. Mills A, Chetty R. Auricular granuloma annulare. A consequence of trauma? *Am J Dermatopathol* 1992; 14: 431-3.
6. Vilanova X, Cardenal C. Granuloma annulare of both pavillions of the ear. *Actas Dermosifiliogr* 1954; 45: 405-6.

doi:10.1684/ejd.2010.0926

Showering reduces atopic dermatitis in elementary school students

Sweat is thought to exacerbate the symptoms of atopic dermatitis (AD) [1, 2]. It is known that the pH of sweat and skin surfaces increases with time [3]; thus, old sweat might cause skin barrier dysfunction and promote infection. Such susceptibility to environmental factors and infection are considered clinical features of AD [4]. Therefore, we hypothesized that rinsing skin surfaces by showering might reduce the severity of atopic dermatitis by decreasing bacteria on the skin surface. It has been reported that showering at school reduces the severity of AD [5, 6]; however, the mechanism has not been determined. We evaluated the effect of showering on skin barrier function and the number of bacteria on affected skin, in elementary school students with AD.

The effects of showering were measured over a 4-week period in September with the approval of the institutional review board. Study subjects (n = 11) were chosen by the presence of AD, and the study was carried out with the consent of a parent or guardian. Students were instructed to rinse skin with a shower or running water during a 20-minute break between the second and third classes every weekday, and to avoid treatment changes during this period. The severity of AD was evaluated using the eczema area and severity index (EASI), as determined by three dermatologists simultaneously. For assessment of the skin barrier function, trans-epidermal water loss (TEWL) and water retaining capacity were evaluated. Estimates of body surface area (BSA) involvement were obtained from the objective severity assessment via AD scoring software. *Staphylococcus aureus* (*S. aureus*) was collected using sterilized filter paper (4 × 4 cm) moistened with sterilized saline and placed against the skin (cubital fossa). The filter paper then was put onto 4 cm of selective medium for *S. aureus*. After incubation at 37 °C for 24 hours, the number of colonies per plate was counted. Determination of shower efficacy was made by dermatologists who visited the school 2 and 4 weeks after the initiation and 2 weeks after the termination of the intervention.

A significant decrease in EASI score was observed at 2 and 4 weeks after the intervention compared with before initiation of the intervention *(figure 1A)*. Disappearance of the eczematous lesion was greatly visible, and a significant decrease in the affected area was observed 4 weeks after initiation and 2 weeks after termination *(figure 1B)*. Unfortunately, the results of TEWL and water retaining capacity showed no specific trend, most likely due to the fact that students participated in athletic activities (causing sweating) just prior to assessment (not shown).

Four weeks after initiation and 2 weeks after termination, a significant decrease in the number of *S. aureus* was observed relative to before initiation of this intervention *(figure 1C)*.

In conclusion, although there are limitations with regard to the number of cases evaluated, study duration, and lack of controlled comparison, we found that showering the skin surface while at school prevented the exacerbation of AD. This favorable effect of showering was produced by a standard shower facility and tap water, and might be mediated by decreasing skin surface bacteria. Of course, optimization of conditions for showering/rinsing in terms of adequate water temperature and the time required for showering should be established in the future. ■

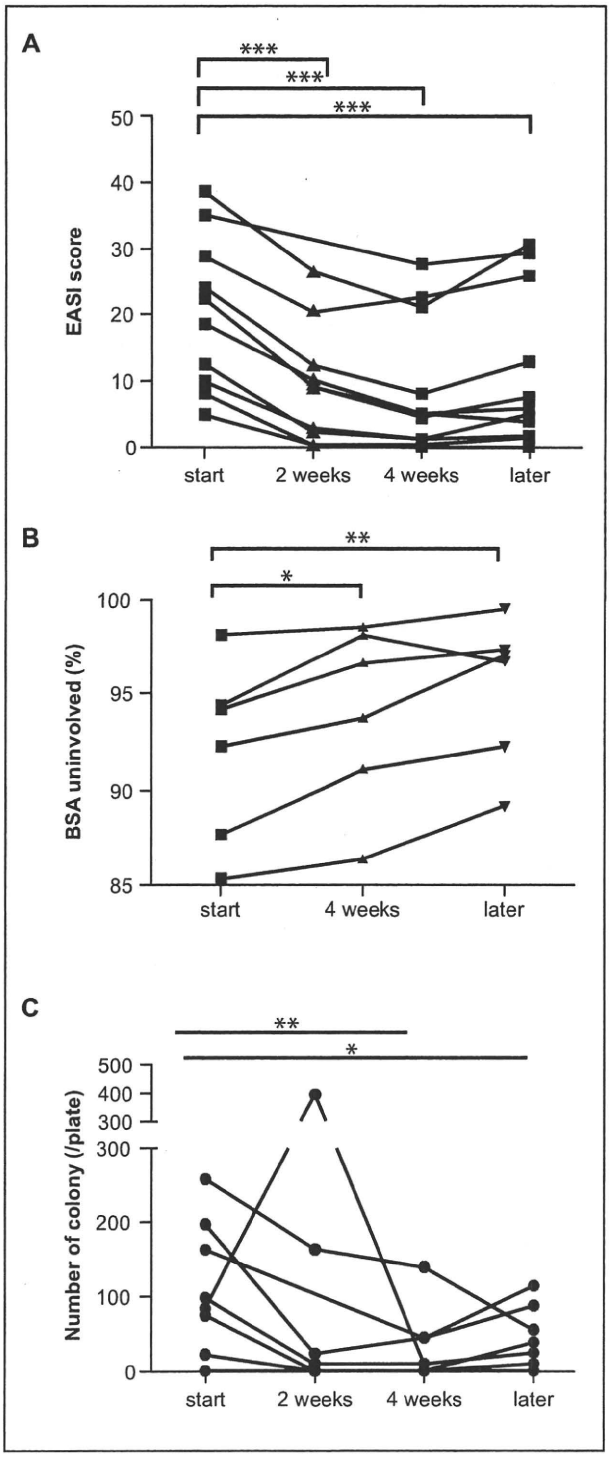

Figure 1. Showering in school improved the severity of atopic dermatitis. **A)** EASI score (n = 11), **B)** Ratio of affected to non-affected area (n = 6), and **C)** Number of colonized *S. aureus* (n = 11). "Start" indicates 2 weeks before initiation of this study. "2 weeks" and "4 weeks" indicate 2 and 4 weeks after initiation of this study, respectively. "Later" indicates 2 weeks after study termination. ***: $p < 0.0001$, ** $p < 0.005$, * $p < 0.05$ (paired *t*-test).

Acknowledgements. *This study was supported by the Health, Labour, and Welfare Ministry of Japan. Conflict of interest: none.*

Department of Dermatology,
Osaka University,
2-2, Yamadaoka,
565-0871 Suita,
Japan
<h-murota@derma.med.osaka-u.ac.jp>

Hiroyuki MUROTA
Aya TAKAHASHI
Megumi NISHIOKA
Saki MATSUI
Mika TERAO
Shun KITABA
Ichiro KATAYAMA

1. Rieg S, Steffen H, Seeber S, *et al*. Deficiency of dermcidin-derived antimicrobial peptides in sweat of patients with atopic dermatitis correlates with an impaired innate defense of human skin in vivo. *J Immunol* 2005; 174: 8003-10.
2. Schmid-Wendtner MH, Korting HC. The ph of the skin surface and its impact on the barrier function. *Skin Pharmacol Physiol* 2006; 19: 296-302.
3. Burry J, Coulson HF, Roberts G. Circadian rhythms in axillary skin surface ph. *Int J Cosmet Sci* 2001; 23: 207-10.
4. Giannetti A, Girolomoni G. Skin diseases with high public health impact. Atopic dermatitis. *Eur J Dermatol* 2007; 17: 566.
5. Mochizuki H, Muramatsu R, Tadaki H, Mizuno T, Arakawa H, Morikawa A. Effects of skin care with shower therapy on children with atopic dermatitis in elementary schools. *Pediatr Dermatol* 2009; 26: 223-5.
6. Katayama I. Evaluation for the effect of moisture retention on prevention and improvement of atopic dermatitis. (in Japanese). *Report of the research for the environmental consideration for determination of complicating factors and reducing the incidence of atopic dermatitis: 2008 The survey results of the ministry of health, labor and welfare of Japan* 2008: 24-6.

doi:10.1684/ejd.2010.0928

AEC syndrome caused by heterozygous mutation in the SAM domain of p63 gene

AEC syndrome is characterized by hypohidrotic ectodermal dysplasia, cleft lip/palate and ankyloblepharon.
A twinborn boy, born prematurely at 35 weeks' gestation, was seen with sparse hair, scaly scalp and the soft and hard palate cleft. He had mid-facial hypoplasia with a narrow nose, a small mouth and a prominent high forehead, and also a fusion of lateral aspects of the eyelid margins (ankyloblepharon) and the external ear anomalies of low-seated small, cupped ears *(figure 1A)*. All finger nails and toe nails were dystrophic and hypospadia was noted.
The early postnatal period was complicated by sepsis, anaemia and development of erosive scalp dermatitis *(figure 1B)*. The skin cultures yielded *Staphylococcus aureus, Klebsiella pneumoniae, Streptococcus agalactiae* and *Candida albicans*, however the patient's dermatitis was only slowly responsive to antimicrobial and antifungal topical and systemic therapy. Recurrent otitis media and tympanic membrane polyps were associated with the ear canal stenosis and there was lacrimal duct obstruction, leading to recurrent conjunctivitis.
His twinborn sister had no signs of ectodermal dysplasia or other abnormalities, but the mother had, besides the facial features, palmoplantar keratoderma, nail, teeth and also, under her wig, hair dysplasia. Her ankyloblepharon and cleft palate had been operated on in early childhood and the family history revealed no other affected family member *(figure 1C)*.

Original Paper

International Archives of Allergy and Immunology

Int Arch Allergy Immunol 2010;153:121–132
DOI: 10.1159/000312629

Received: September 28, 2009
Accepted after revision: December 3, 2009
Published online: April 21, 2010

Olopatadine Hydrochloride Improves Dermatitis Score and Inhibits Scratch Behavior in NC/Nga Mice

Hiroyuki Murota[a] Mostafa Abd El-latif[a] Tadafumi Tamura[b] Toru Amano[b] Ichiro Katayama[a]

[a]Department of Dermatology, Course of Integrated Medicine, Graduate School of Medicine, Osaka University, Osaka, [b]Research Division, Pharmaceutical Research Laboratories, Kyowa Hakko Kirin Co., Ltd., Shizuoka, Japan

Key Words

Olopatadine hydrochloride · Atopic dermatitis · Model animal · Neurite outgrowth · Inflammation · Itch

Abstract

Background: Control of itch is an important issue in the treatment of atopic dermatitis (AD). Itch is mediated by a variety of pruritogens, including histamine, and promoted by neurite outgrowth in the epidermis of AD patients, probably due to the release of nerve growth factor. ***Objectives:*** We investigated the effects of orally administered olopatadine hydrochloride (olopatadine) on itching, itching mediators, and neuritogenic action in a mouse model. ***Materials and Methods:*** NC/Nga mice were treated topically with *Dermatophagoides farinae* body (Dfb) extract twice weekly for 4 weeks to induce AD-like lesions. They were concomitantly given oral olopatadine, distilled deionized water, or topical tacrolimus during the last 2 weeks. ***Results:*** Olopatadine significantly suppressed scratching, improved the dermatitis score, inhibited neurite outgrowth, and decreased the elevated inflammatory markers, growth factors and histamine content in the lesional skin, and serum concentration of Dfb-specific IgE. Notably, olopatadine treatment increased semaphorin 3A expression in the epidermis. ***Conclusions:*** Our study confirms the pleiotropic effects of olopatadine, i.e. inhibition of inflammation and neurite extension into the epidermis.

Introduction

Itch is a major symptom in allergic skin diseases that affects patients' quality of life [1]. Itch is induced by specific nonmyelinated C-fiber stimulation and the magnitude of itch is modulated by changes in stimulus frequency [2]. In atopic dermatitis (AD) skin lesions, increased epidermal nerve fiber density is frequently observed [3–5]. Substances found to be pruritogenic in AD include histamine, serotonin, prostaglandins, bradykinin, proteinases, opioids, cytokines and leukotrienes [2, 6–13]. Histamine, in particular, has been implicated as a cause of itch, inflammation and tissue remodeling in AD [7, 14–17], primarily through H_1 receptor activation [7]. Histamine

Hiroyuki Murota and Mostafa Abd El-latif contributed equally to this work.

KARGER

Fax +41 61 306 12 34
E-Mail karger@karger.ch
www.karger.com

1018–2438/10/1532–0121$26.00/0

Accessible online at:
www.karger.com/iaa

Correspondence to: Dr. Hiroyuki Murota, Department of Dermatology
Course of Integrated Medicine, Graduate School of Medicine, Osaka University
2-2 Yamadaoka, Suita, Osaka 565-0871 (Japan)
Tel. +81 668 79 3031, Fax +81 668 79 3039
E-Mail h-murota@derma.med.osaka-u.ac.jp

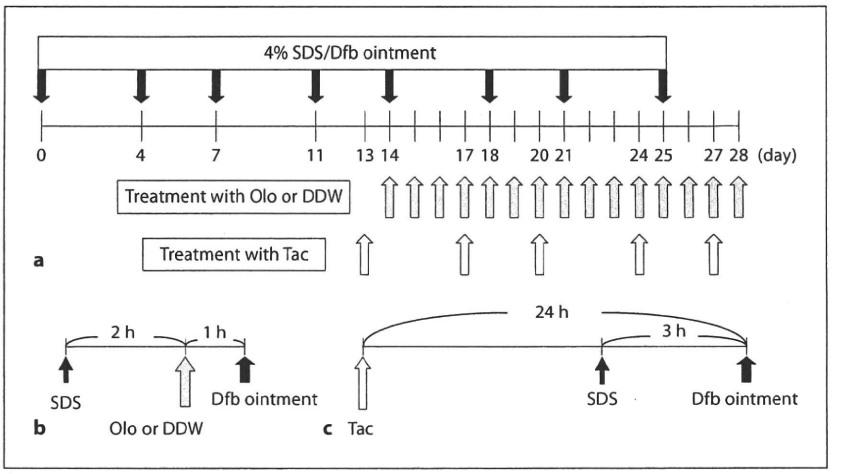

Fig. 1. Schematic illustration of the protocol. **a** Dermatitis was induced by topical application of 100 mg Dfb ointment twice a week until day 25. Another group was comprised of animals that were treated with SDS alone (sham). After 2 weeks of Dfb application, olopatadine (Olo, 3 and 10 mg/kg/day) or DDW was administered orally every day from day 14 to 28. Tacrolimus (Tac) ointment (100 mg/) was applied to the back skin twice a week. **b** Administration schedule of olopatadine or DDW and Dfb ointment on the same day. **c** Tacrolimus treatment was performed 24 h before application of Dfb ointment.

is stored in dermal mast cells and keratinocytes while H_1 and H_2 receptors are present on sensory nerve fibers. Along with neuronal depolarization, neuropeptides such as substance P are released from nerve endings. Substance P elicits scratching behavior, possibly mediated by histamine through degranulation of mast cells [18].

NC/Nga mice develop AD-like skin lesions and increased plasma IgE under conventional stimulation [19]. These symptoms can also be elicited under specific pathogen-free (SPF) conditions using *Dermatophagoides farinae* extract [20]. Treated NC/Nga mice react by scratching [21], and are therefore used as a model for evaluating the antipruritic effect of certain agents [22]. Pruritus in this strain is partly explained by neurite outgrowth in the epidermis due to increased expression of nerve growth factor (NGF) [23], which is also observed in AD-like skin lesions. The antipruritic effect of dexamethasone, tacrolimus, chlorpheniramine maleate, cyproheptadine hydrochloride and bepotastine besilate has been evaluated via the scratching behavior of NC/Nga mice [22, 24].

Olopatadine is a histamine H_1 receptor antagonist and has been approved in Japan as an oral drug for the treatment of allergic rhinitis, chronic urticaria, eczema/dermatitis, prurigo, pruritus, psoriasis vulgaris, and erythema multiforme [25]. Worldwide, olopatadine ophthalmic solution, which inhibits the proinflammatory activity of conjunctival mast cells, is an effective therapy for allergic conjunctivitis [26]. An olopatadine nasal spray was recently launched for the treatment of nasal allergy symptoms [27]. It has been reported that olopatadine attenuates (1) the elevation of various inflammatory cytokines in skin lesions, and (2) the scratching behavior in a mouse model of chronic contact dermatitis induced by repeated hapten challenge [28, 29]. Furthermore, olopatadine accelerates the recovery of skin barrier function [30]. We evaluated the antineuritogenic and antipruritic effects of olopatadine in NC/Nga mice with dermatitis. We used topical application of tacrolimus, which suppresses intraepidermal neurite outgrowth and scratch behavior [31], as a positive control.

Materials and Methods

Animals

Female NC/Nga Tnd mice (NC/Nga mice) were purchased from Charles River Japan (Kanagawa, Japan) and used at 10 weeks of age. Female Wistar rats were purchased from Japan SLC (Shizuoka, Japan) and used at 6 weeks of age. The animals were housed in the SPF animal facility at 19–25°C and 30–70% humidity, with 12-hour light/dark cycles and access to food and water ad libitum. The animals were cared for according to the ethical guidelines of the Institutional Animal Care and Use Committee of Osaka University.

Drugs

Olopatadine (Kyowa Hakko Kirin, Tokyo, Japan) was synthesized at Yokkaichi Plant, Kyowa Hakko Kirin (Mie, Japan) and dissolved in distilled deionized water (DDW). Tacrolimus ointment (Protopic® Ointment 0.1%) was purchased from Astellas Pharma (Tokyo, Japan). *D. farinae* body (Dfb) ointment was prepared by Biostir (Kobe, Japan).

Induction of Dermatitis

Figure 1 illustrates the details of this protocol. Dermatitis was induced in NC/Nga mice according to the method of Yamamoto et al. [20, 32]. On day 0, the dorsal region of mice was shaved under anesthesia. Dermatitis was induced by topical application of 100 mg Dfb ointment on the shaved dorsal skin and both sur-

faces of both ears for 4 weeks (fig. 1a). Barrier disruption was achieved by 150 μl of 4% sodium dodecyl sulfate (SDS) treatment 3 h before application of Dfb ointment (fig. 1b, c). These procedures were repeated twice per week until day 25. Three days following the last application (day 28), the mice were sacrificed and histological changes evaluated. An additional group comprised animals that were treated with SDS alone (sham group, n = 6).

Inhibition of Dermatitis by Olopatadine or Tacrolimus Ointment

Not all of the mice developed dermatitis after Dfb application. To exclude the results from dermatitis-free mice, we initiated Dfb application to 48 mice. After 2 weeks of Dfb application, we selected 40 mice in descending order of severity of dermatitis. The lowest dermatitis score in those 40 mice was 3. To avoid the influence of the starting number of mice, the affected mice were divided into 4 equal groups as follows: group 1 received 3 mg/kg/day olopatadine (n = 10) and group 2 received 10 mg/kg/day olopatadine (n = 10) orally, daily from day 14 to 28. Group 3 received tacrolimus ointment (100 mg), applied to the back skin twice per week (days 13, 17, 20, 24, and 27; n = 10). DDW served as a control (group 4; n = 10). If the administration of olopatadine or DDW and application of Dfb ointment was performed on the same day, the former was performed 1 h before the Dfb treatment (fig. 1b). Tacrolimus treatment was performed 24 h before the application of Dfb ointment (fig. 1c). Two mice from the tacrolimus-treated group died unexpectedly for unknown reasons. On the final day (day 28), 24 h after the tacrolimus treatment and 1 h after olopatadine or DDW administration, the final evaluation was performed.

Evaluation of Dermatitis

The severity of dermatitis was evaluated weekly. Observations of erythema/hemorrhage, scarring/dryness, edema, excoriation/erosion, and scaling/dryness were scored as 0 (no symptoms), 1 (weak), 2 (mild), and 3 (severe) [20]. The sum of the individual scores was taken as the dermatitis score (total score: minimum 0, maximum 12). The severity of dermatitis was scored independently by three researchers.

Observation of Scratching Behavior

The mice were placed in compartments (7 × 77 × 15 cm) of observation cages for 60 min of habituation. Their behavior was recorded by an unmanned digital video camera (Panasonic, Osaka, Japan) for 90 min. The number of scratching episodes was counted in a blinded fashion. A series of scratching movements with the hind paw was considered as one scratching episode as described previously [29].

Histological Analysis

Skin biopsies were obtained from between the shoulder blades of all mice. Skin samples were fixed in 4% paraformaldehyde at 4°C overnight (O/N). Four-micrometer, paraffin-embedded sections were stained with hematoxylin and eosin (HE).

Immunohistochemical Staining for Anti-Protein Gene Product 9.5

Specimens were fixed in 4% paraformaldehyde O/N and rinsed with phosphate-buffered saline (PBS) containing 10, 15, and finally 20% sucrose. Tissues were embedded with OCT compound, and frozen in liquid nitrogen. Frozen tissues were cut at 30 μm and air-dried at room temperature for 1 h. Sections were washed in three 5-min changes of PBS and blocked with blocking buffer (5% bovine serum albumin, 0.1% Triton X-100 in PBS) at room temperature for 30 min, followed by incubation with Protein Gene Product 9.5 (PGP9.5) antibody (1:500 dilution) (Chemicon, Temecula, Calif., USA) at 4°C O/N. Subsequently, sections were washed in three changes of PBS and incubated with Alexa Fluor® 488-conjugated anti-rabbit antibody (1:500 dilution) (Molecular Probes, Eugene, Oreg., USA) at 4°C O/N. Images of immunolabeled sections were captured with a BZ-8000 microscope (Keyence, Osaka, Japan).

Quantification of Intraepidermal Neurites

To quantify intraepidermal neurite outgrowth, we modified the method of Tominaga et al. [23]. Specimens, obtained with a 5-mm diameter biopsy punch, were stained with anti-PGP9.5 antibody, and in confocal microscopic analysis, 1.5-μm optical sections were scanned through the *z*-plane (thickness 30 μm). Three-dimensional reconstruction was performed using software for the BZ-8000. For counting neurite numbers, at least 27 confocal images were merged per group in each experiment. The number of intraepidermal neurites per 1.6×10^5 μm^2 in the central portion of the biopsy was hand-counted independently by two researchers.

Semiquantitative Reverse-Transcriptase-Polymerase Chain Reaction

Skin samples were incubated O/N with 4% dispase (Invitrogen, Carlsbad, Calif., USA). The epidermis was separated from the dermis, and total RNA from the epidermis or dermis was extracted with an SV Total RNA Isolation kit (Promega, Madison, Wisc., USA) according to the manufacturer's protocol. First-strand cDNA was synthesized with an AffinityScript™ QPCR cDNA synthesis kit (Stratagene, La Jolla, Calif., USA) using oligo dT primers, followed by amplification of the cDNA for 25 cycles. The following oligonucleotide primers were used for the reverse-transcriptase-polymerase chain reaction (RT-PCR): for semaphorin 3A (sema3A): sense 5′-AGCCTTGAAGAGAGAATCATCTAT-3′, antisense 5′-AACTCGTGGGTCCTCCTGTTTCTA-3′, for NGFβ1: sense 5′-ATAAAGGTTTTGCCAAGGAC-3′, antisense 5′-CACGGGGTGAGTGGAGTCTC-3′, for β-actin: sense 5′-TGTTACCAACTGGGACGACA-3′, antisense 5′-GGGGTGTTGAAGGTCTCAAA-3′. Band intensity was measured using ImageJ software, and the relative value of sema3A and NGFβ1 to β-actin was calculated.

Measurement of Histamine, Substance P, NGF, Amphiregulin, IL-1β, TNF-α, IL-6, GM-CSF, E-Selectin, IFN-γ and IL-4 in Skin Lesions

Skin samples were excised 3 days after the final Dfb application. Samples were minced and homogenized in ice-cold PBS containing a protease inhibitor (Complete; Roche Diagnostics, Mannheim, Germany) with a Polytron tissue homogenizer. Precipitate was removed by centrifugation, and supernatant was collected. Histamine (CIS bio, Gif-sur-Yvette, France); substance P (Cayman, Ann Arbor, Mich., USA); NGF (Promega); amphiregulin, IL-1β, TNF-α, IL-6, GM-CSF and E-selectin (R&D Systems, Minneapolis, Minn., USA); IFN-γ and IL-4 (Thermo Scientific, Rockford, Ill., USA) and protein (Thermo Scientific) concentrations were analyzed with an assay kit according to the manufacturer's protocol.

Measurement of Serum Total IgE and Specific IgE to Dfb

Blood samples were collected under anesthesia 3 days after the last Dfb application. Total IgE level was determined using a mouse ELISA kit (Biosciences, San Jose, Calif., USA), according to the manufacturer's protocol. Specific IgE to Dfb was evaluated using passive cutaneous anaphylaxis, according to the method of Yamamoto et al. [32]. Wistar rats were used as recipients and sensitized with intradermal injections of 50 μl of serially diluted sera into the shaved dorsal skin. The rats were challenged 24 h later by intravenous injections of 0.5 ml saline containing 1 mg Dfb and 5 mg Evans Blue. Thirty minutes later, the animals were sacrificed by exsanguination under deep plane anesthesia. The pigmented area was measured from the inner side of the skin. An area >5 mm in diameter was regarded as a positive reaction, and the antibody titer was determined.

Statistical Analysis

Data are presented as means ± SEM. Student's t test or the Aspin-Welch test following the F test was used for the analysis of differences between two groups. Multiple comparisons among treatment groups were assessed by one-way ANOVA, followed by Dunnett's test, or the Kruskal-Wallis test followed by the Steel test. Statistical analysis of the dermatitis scores was performed by the Wilcoxon rank sum for analysis of differences between two groups, and by the Steel test for multiple comparisons among treatment groups. In all tests, $p < 0.05$ was considered statistically significant.

Results

Olopatadine Improved Dermatitis in NC/Nga Mice

To validate the ability of olopatadine to improve dermatitis in NC/Nga mice, olopatadine was given orally and tacrolimus was applied topically to NC/Nga mice with Dfb-induced skin lesions (fig. 1). Dfb treatment for 2 weeks elicited severe dermatitis. Although the dermatitis scores of the DDW group (control group) increased, those of the olopatadine (10 mg/kg/day) group significantly decreased beginning 1 week after the initial administration (day 21). After 2 weeks (day 28) the dermatitis score of the olopatadine group showed a significant improvement while the tacrolimus group failed to improve (fig. 2). The gross appearance of the involved skin in the control group showed dryness, desquamation, erythema, crusts and excoriation; those manifestations were relatively attenuated in the olopatadine and tacrolimus groups (fig. 3a). A pronounced effect was observed in the olopatadine (10 mg/kg) group. Histopathological examination of the control group revealed severe acanthosis and the presence of an inflammatory cell infiltrate (fig. 3a). These abnormal findings were partially improved in the olopatadine and tacrolimus groups (fig. 3a). It is notable that acanthosis was significantly improved in the olopatadine (10 mg/kg) group (fig. 3b).

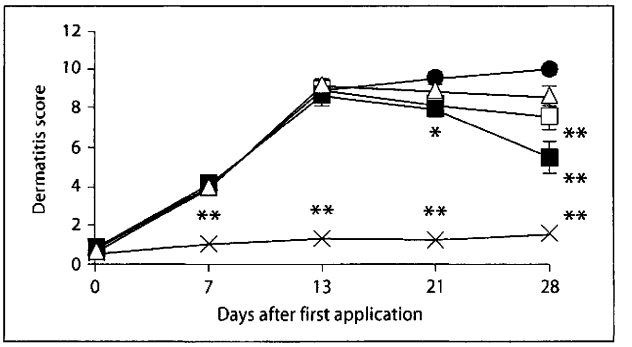

Fig. 2. Effect of olopatadine and tacrolimus ointment on the established dermatitis model. Dfb treatment was carried out for 2 weeks prior to administration of 3 mg/kg/day of olopatadine (□) (n = 10), 10 mg/kg/day of olopatadine (■) (n = 10), DDW (●) (n = 10), or topical treatment with tacrolimus (△) (n = 8). Sham treatment (×) (n = 6) was used as a negative control. Each point represents the mean ± SEM of 6–10 mice. * $p < 0.05$, ** $p < 0.01$: significantly different from the control group.

Olopatadine Diminished Scratching in NC/Nga Mice

Scratching exacerbates dermatitis. To assess the effect of olopatadine on scratching, 90-min videos were obtained of mice on the final day (fig. 4). As expected, the number of scratching episodes was significantly higher in the control group than in the sham group. The olopatadine groups (3 and 10 mg/kg/day) showed the lowest numbers of scratching episodes (inhibition ratios of 66.7 and 86.5%, respectively) (fig. 4a). The tacrolimus group did not show any trend toward improvement in scratching behavior (fig. 4a). Next, we measured the amount of itching-related factors, such as histamine and substance P, in affected skin. Histamine levels were significantly lower in the olopatadine groups (fig. 4b). The olopatadine groups (3 and 10 mg/kg/day) exhibited a reduction of 22.3 and 59.4% in substance P concentration compared with the control group; this difference is not statistically significant, however (fig. 4c). The levels of these factors were unaltered in the tacrolimus group (fig. 4b, c).

Olopatadine Decreased Intraepidermal Neurite Formation

Intraepidermal neurite outgrowth may contribute to pruritus in affected skin [23]. Thus, we hypothesized that olopatadine would inhibit intraepidermal neurite outgrowth in Dfb evoked dermatitis in NC/Nga mice. To test this hypothesis, skin sections were immunolabeled with PGP9.5 and substance P. Since not every PGP9.5-positive nerve fiber was colabeled with substance P (fig. 5a),

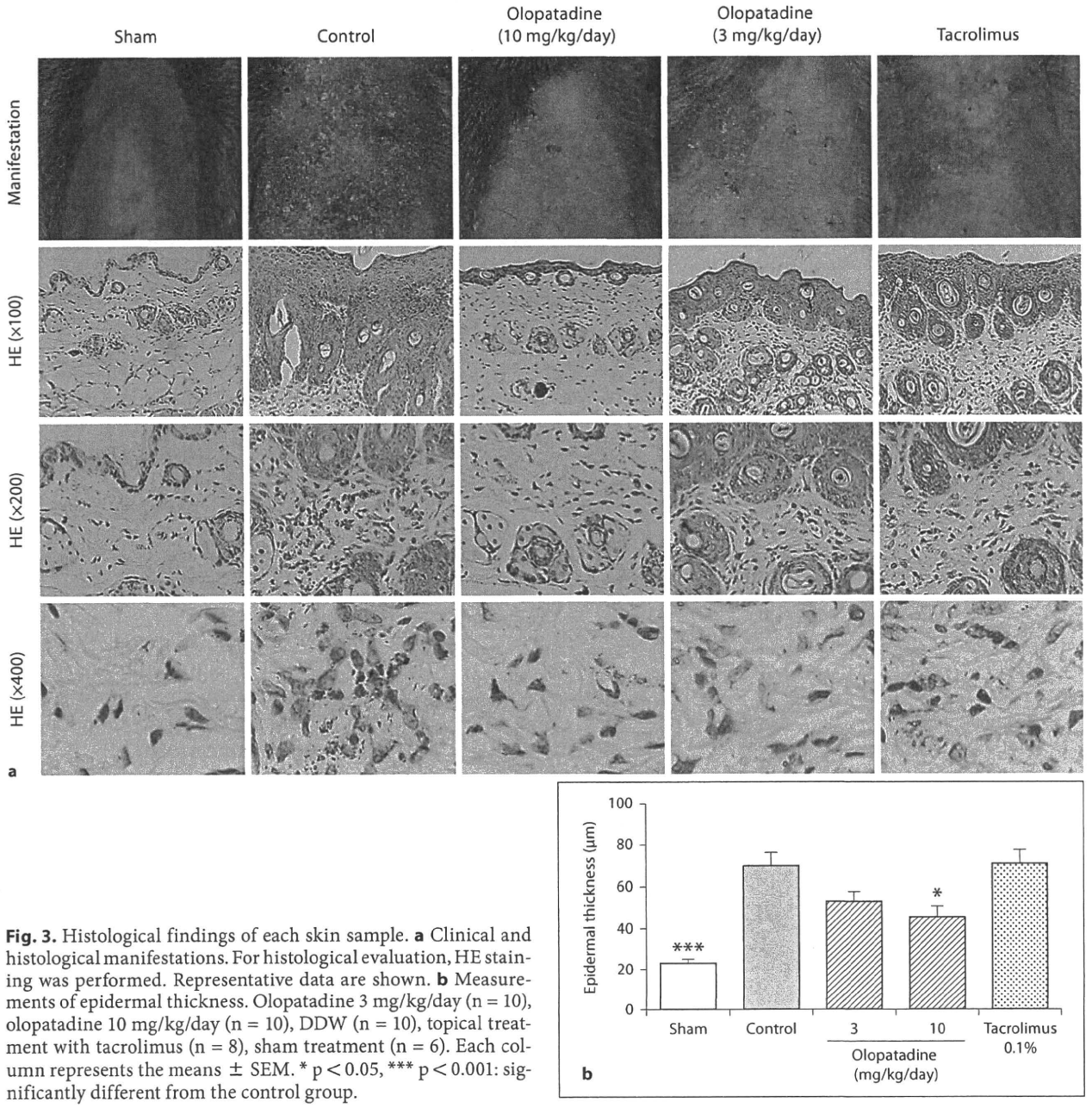

Fig. 3. Histological findings of each skin sample. **a** Clinical and histological manifestations. For histological evaluation, HE staining was performed. Representative data are shown. **b** Measurements of epidermal thickness. Olopatadine 3 mg/kg/day (n = 10), olopatadine 10 mg/kg/day (n = 10), DDW (n = 10), topical treatment with tacrolimus (n = 8), sham treatment (n = 6). Each column represents the means ± SEM. * $p < 0.05$, *** $p < 0.001$: significantly different from the control group.

PGP9.5-positive intraepidermal neurites were counted. The number of PGP9.5-positive neurites was more markedly increased in the control group than in the sham group, olopatadine groups or tacrolimus group (fig. 5a). Strikingly, the number of intraepidermal neurites was significantly decreased in the olopatadine and the tacrolimus groups (fig. 5b).

Olopatadine Affected NGF, Amphiregulin, and Sema3A Expression in Skin

The results in figure 4 suggest that olopatadine affects the expression of certain growth factors or axon guidance molecules in the skin. Predictably, NGF protein expression was significantly lower in the lesional skin of the olopatadine and the tacrolimus groups than in the con-

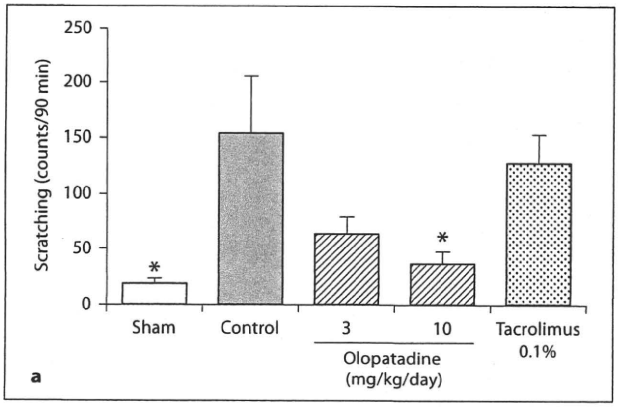

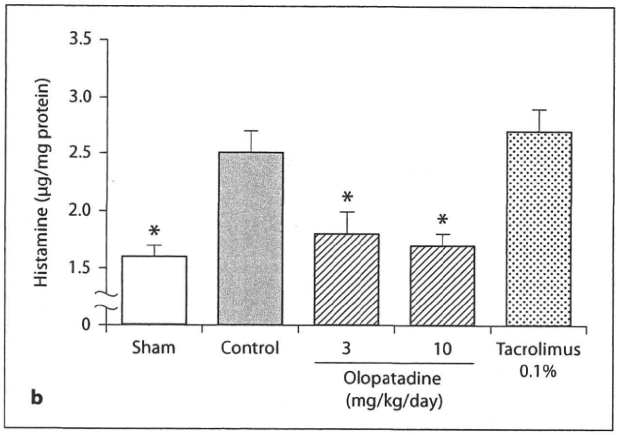

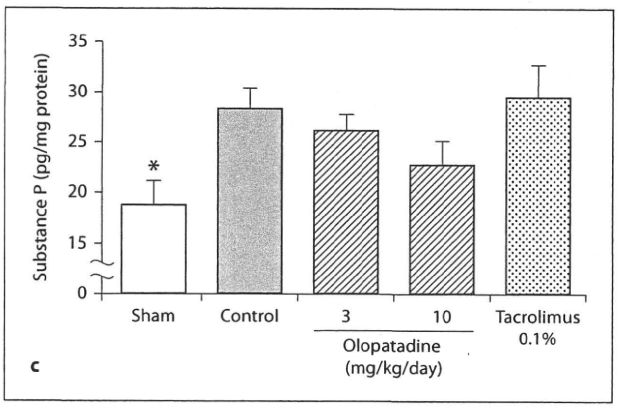

Fig. 4. Effect of olopatadine on scratch behavior and on the histamine and substance P content in the skin. **a** Number of scratching events. **b**, **c** Histamine and substance P contents in the skin samples. Each point represents the mean ± SEM. * $p < 0.05$: significantly different from the control group. Olopatadine 3 mg/kg/day (n = 10), olopatadine 10 mg/kg/day (n = 10), DDW (n = 10), topical treatment with tacrolimus (n = 8), sham treatment (n = 6).

trol group (fig. 6a). The amphiregulin content, which is thought to be related to neurite outgrowth [23], was also decreased in the lesional skin of the olopatadine groups (fig. 6b). Furthermore, semiquantitative PCR analysis was performed to detect sema3A and NGFβ1 in dermal and epidermal samples. The results revealed increased expression of NGFβ1-mRNA in the epidermis, which was significantly decreased in the olopatadine and tacrolimus groups (fig. 6c). Interestingly, sema3A mRNA expression, a potent inhibitor of neurite outgrowth, significantly increased in the epidermis of the high-dose olopatadine (10 mg/kg/day) group (fig. 6d). Moreover, NGFβ1 and sema3A expression was not detected in all dermal samples (data not shown). These results indicate that olopatadine inhibits neurite outgrowth by regulating the expression of such factors in the epidermis but not in the dermis. Similarly to the olopatadine group, the tacrolimus group also exhibited significantly decreased NGF and amphiregulin expression (fig. 6a–c), with no effect on sema3A expression (fig. 6d).

Effect of Olopatadine on the Levels of Inflammatory Markers in the Skin

Reduced numbers of inflammatory cell infiltrates were observed in the affected skin of the olopatadine groups (fig. 3). Olopatadine might thus reduce the inflammatory reaction. In support of this assumption, the expression of inflammatory markers such as IL-1β, TNF-α, IL-6, GM-CSF and E-selectin in the skin significantly decreased in the olopatadine groups (table 1). The tacrolimus group also showed significantly reduced levels of inflammatory markers (table 1). IFN-γ and IL-4 levels were not affected by olopatadine or tacrolimus treatment.

Olopatadine Decreased Serum Concentrations of Total and Dfb-Specific IgE

As NC/Nga mice develop chronic dermatitis associated with IgE hyperproduction [19], we also examined serum concentrations of both total and Dfb-specific IgE. Compared with the control group, total IgE was reduced, although not statistically significantly, by 6.4 and 31.9%, respectively, in the serum of the olopatadine (3 and 10 mg/kg/day) groups (fig. 7a). Unexpectedly, the tacrolimus group also exhibited an increased serum concentration of total IgE (fig. 7a). Next, we focused on the serum concentration of antigen-specific IgE. Since there is no commercially available Dfb-specific IgE ELISA, we performed the passive cutaneous anaphylaxis test to determine the Dfb-specific IgE titer. The Dfb-specific IgE titer

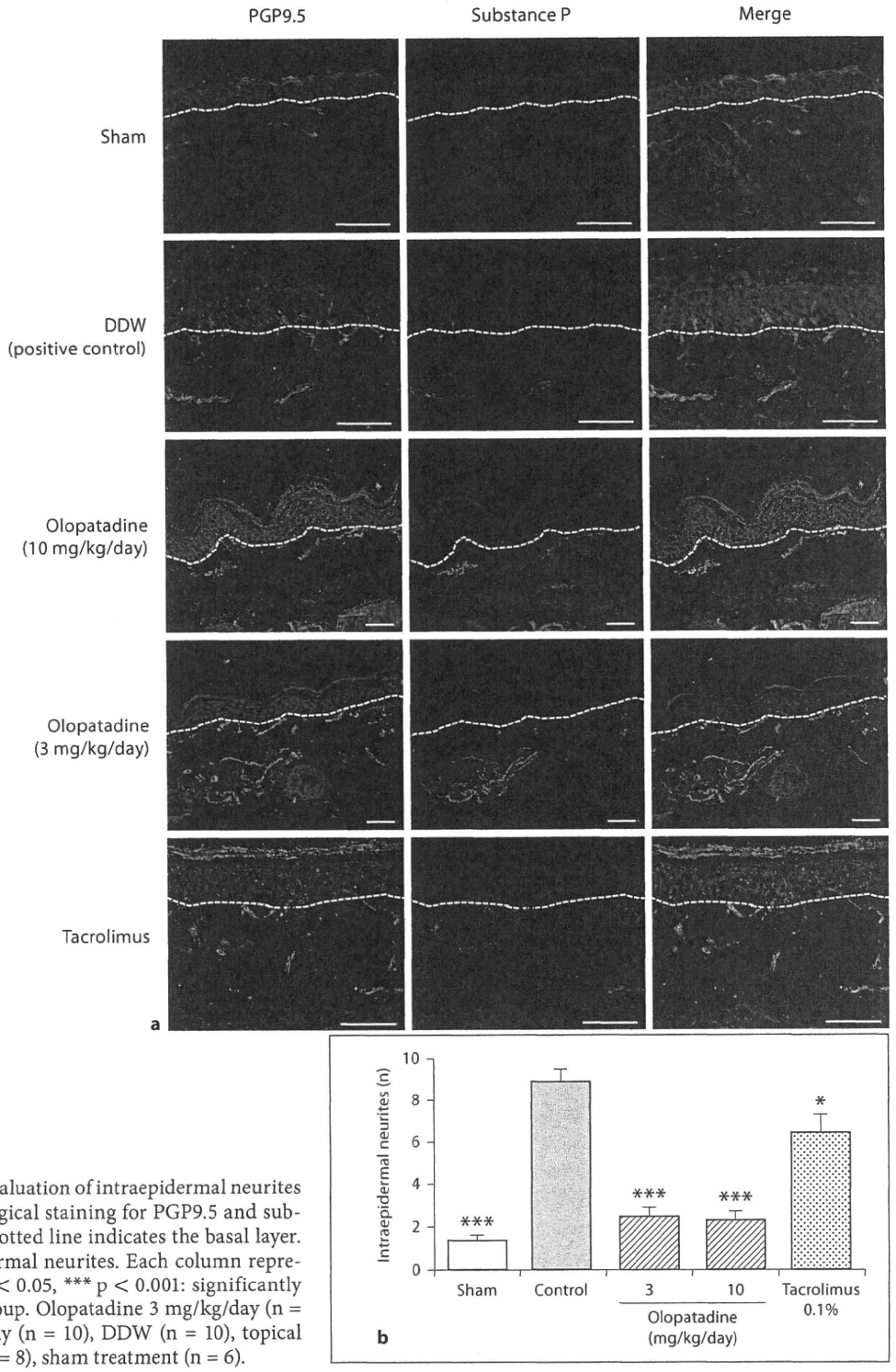

Fig. 5. Immunohistological evaluation of intraepidermal neurites outgrowth. **a** Immunohistological staining for PGP9.5 and substance P. Scale bar: 50 μm. Dotted line indicates the basal layer. **b** PGP9.5-positive intraepidermal neurites. Each column represents the mean ± SEM. * $p < 0.05$, *** $p < 0.001$: significantly different from the control group. Olopatadine 3 mg/kg/day (n = 10), olopatadine 10 mg/kg/day (n = 10), DDW (n = 10), topical treatment with tacrolimus (n = 8), sham treatment (n = 6).

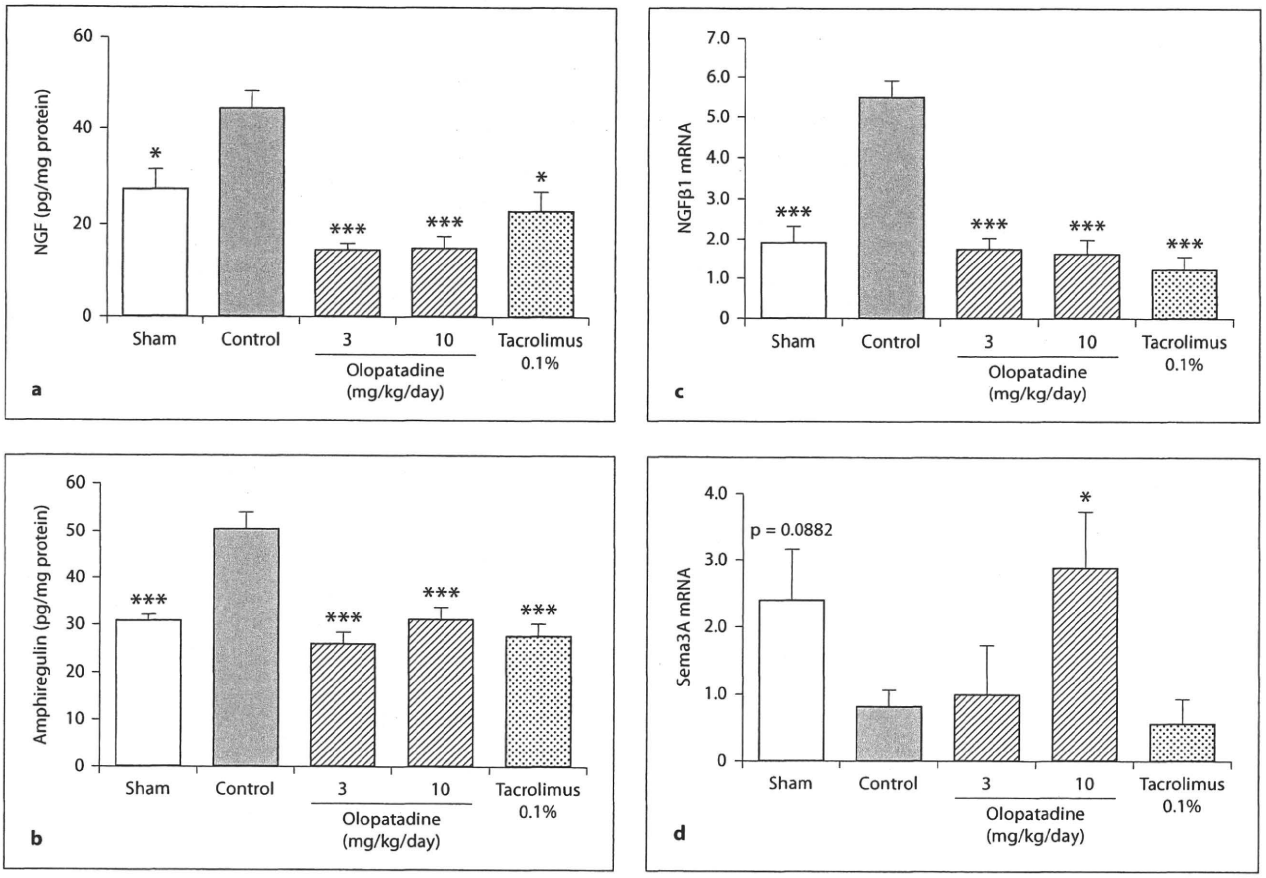

Fig. 6. a, b NGF and amphiregulin protein content in the lesional skin (whole skin). Olopatadine 3 mg/kg/day (n = 10), olopatadine 10 mg/kg/day (n = 10), DDW (n = 10), topical treatment with tacrolimus (n = 8), sham treatment (n = 6). **c, d** Semi-quantitative PCR results for the mRNA expression level of NGFβ1 and sema 3A in the epidermis. Five animals per group. Each column represents the mean ± SEM. * $p < 0.05$, *** $p < 0.001$: significantly different from the control group.

Table 1. Inflammatory cytokines and adhesion molecules in the lesional skin (whole skin)

	Sham	Control	Olopatadine		Tacrolimus, 0.1%
			3 mg/kg/day	10 mg/kg/day	
IL-1β	6.2 ± 1.0***	13.6 ± 1.2	8.2 ± 0.6	4.9 ± 0.5***	5.9 ± 0.6***
TNF-α	73.6 ± 8.9***	102.7 ± 4.3	74.0 ± 8.5**	47.7 ± 4.3***	83.1 ± 8.3
IL-6	24.8 ± 1.2*	32.5 ± 3.1	26.0 ± 2.9	19.6 ± 2.5**	21.6 ± 2.0*
GM-CSF	12.1 ± 1.7*	16.6 ± 0.7	11.7 ± 1.3**	10.8 ± 0.9***	11.7 ± 1.0**
E-selectin	135.8 ± 16.6***	386.0 ± 23.5	220.2 ± 11.8***	151.5 ± 8.0***	254.3 ± 19.2**
IFN-γ	2,561.9 ± 265.5	1,683.0 ± 76.6	1,485.5 ± 121.5	1,842.1 ± 118.4	1,982.4 ± 155.9
IL-4	176.8 ± 21.9*	133.2 ± 8.1	119.3 ± 12.3	142.2 ± 12.5	154.4 ± 15.9

Each column represents the means ± SEM. * $p < 0.05$, ** $p < 0.01$, *** $p < 0.001$: significantly different from the control group.
Sham treatment (n = 6), DDW (n = 10), olopatadine 3 mg/kg/day (n = 10), olopatadine 10 mg/kg/day (n = 10), topical treatment with tacrolimus (n = 8).

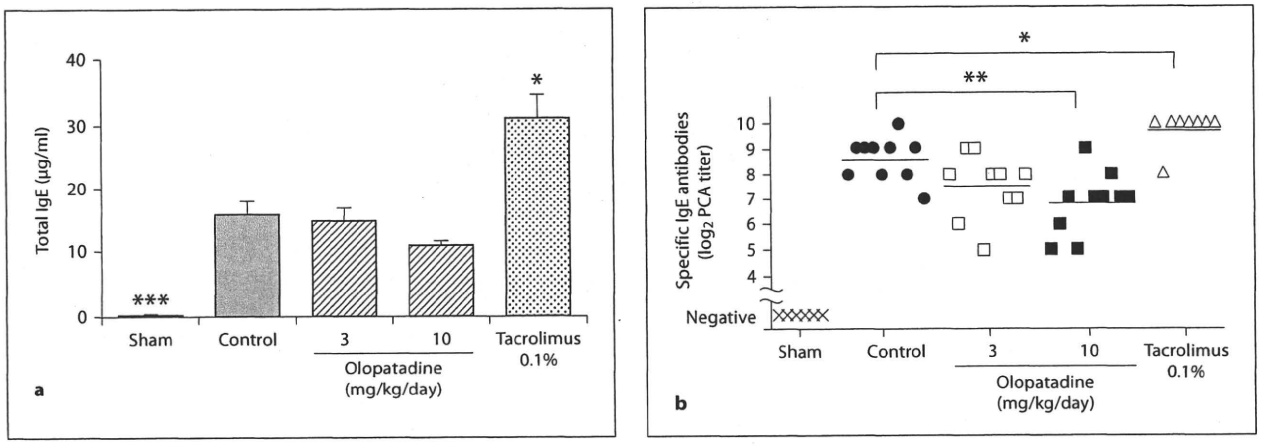

Fig. 7. Serum total IgE and Dfb-specific IgE levels. **a** Total IgE levels were determined by ELISA assay. **b** Specific IgE against Dfb was evaluated using passive cutaneous anaphylaxis. The Evans blue-stained area was measured from the inner side of the skin. An area >5 mm in diameter was regarded as a positive reaction, and the antibody titer was indicated. Each column represents the mean ± SEM. * $p < 0.05$, ** $p < 0.01$, *** $p < 0.001$: significantly different from the control group. Olopatadine 3 mg/kg/day (n = 10), olopatadine 10 mg/kg/day (n = 10), DDW (n = 10), topical treatment with tacrolimus (n = 8), sham treatment (n = 6).

in the high-dose olopatadine (10 mg/kg/day) group was significantly lower than in the control group (fig. 7b). Unexpectedly, the Dfb-specific IgE titer in the tacrolimus group also was significantly higher than in the control group; the cause of this difference is unknown (fig. 7b).

Discussion

Histamine and H_1 receptor-mediated events have been found to play a key role in the development of eczematous lesions in experimental dermatitis in mice [24, 28, 33]. Seike et al. [33] reported that histamine-deficient (histidine decarboxylase gene knockout) mice failed to develop diphenylcyclopropenone (DCP)-induced contact dermatitis, and this phenomenon was corrected by treatment with an H_1 receptor agonist. Loratadine, an H_1 receptor antagonist, administered intraperitoneally from the start of the DCP challenge (twice daily administration for 3 weeks), prevented the development of eczema [33]. It is worth noting that in the present study an orally administered H_1 receptor antagonist improved the Dfb-evoked dermatitis in NC/Nga mice.

How does olopatadine improve dermatitis symptoms? Previous reports provided evidence for the pleiotropic effects of olopatadine: amelioration of the damaged skin barrier function [34], stabilization of mast cells [35], inhibition of monocyte migration [36], and improvement of inflammation and scratch behavior in oxazolone-evoked chronic dermatitis [28, 29]. Of course, the therapeutic effects of olopatadine (reduced inflammatory cell infiltrates, cytokines and histamine) might result from the complex combination of these events. However, we focused on the cause of scratching behavior, especially on intraepidermal neurite outgrowth in this mouse model.

It has been reported that the increased number of peripheral nerve fibers might contribute to reducing the itch sensation threshold in AD and NC/Nga mice [3, 23, 27]. Tominaga et al. [23] formulated the hypothesis that increased NGF and amphiregulin production and abnormal expression of cell-cell junctional molecules in the epidermis might cause abnormal neurite elongation into the epidermis of NC/Nga mice. Furthermore, these authors also reported decreased sema3A production in the lesional epidermis in AD [37, 38]. In our study, the skin samples from NC/Nga mice with Dfb-evoked dermatitis (control group) also showed increased tissue concentration of NGF and amphiregulin, which were significantly decreased following administration of olopatadine and tacrolimus (fig. 5a, b). Since the olopatadine and tacrolimus groups had significantly decreased expression of inflammatory markers such as IL-1β, IL-6, GM-CSF and E-selectin, we assumed that both suppression of inflammation and decreased expression of NGF and amphireg-